1993

Numerical analysis of the photo-dissociation/radical oxidation of formaldehyde by ultraviolet light in a photolytic reactor.

Fetter, Robert O.

NUMERICAL ANALYSIS OF THE PHOTO-DISSOCIATION/RADICAL OXIDATION OF FORMALDEHYDE BY ULTRAVIOLET LIGHT IN A PHOTOLYTIC REACTOR

1993

ROBERT O. FETTER

The Pennsylvania State University

The Graduate School

NUMERICAL ANALYSIS OF THE PHOTO-DISSOCIATION/RADICAL OXIDATION OF FORMALDEHYDE BY ULTRAVIOLET LIGHT IN A PHOTOLYTIC REACTOR

An Engineering Report in

Mechanical Engineering

by

Robert O. Fetter

Submitted in Partial Fulfillment
of the Requirements
for the Degree of

Master of Science, Mechanical Engineering

December 1993

We approve the engineering report of Robert O. Fetter.

TABLE OF CONTENTS

LIST OF FIGURES

LIST OF TABLES

ACKNOWLEDGEMENTS

I would like to extend my sincere gratitude to Professor R. J. Heinsohn whose expertise in the area of air pollution control and unrelenting support allowed me to complete this research on a difficult time schedule and also to the United States Navy for giving me the opportunity to study at Penn State University.

In addition, I wish to recognize the outstanding assistance rendered by Professor L. L. Pauley whose expertise in numerical methods allowed this numerical model to be completed very rapidly. Finally, fellow graduate student Pete Wilson is also acknowledged for his assistance.

Chapter 1

INTRODUCTION

The release of volatile organic compounds (VOC's)into the atmosphere has come under fire by the Environmental Protection Agency (EPA) and state regulatory agencies in the past several years. These releases come from a wide variety of sources from gasoline filling stations to industrial and military operations. There are also countless natural sources of VOC's including volcanos and forest fires. Environmental groups have had a great influence on government agencies resulting in the enactment of numerous statutes and regulations to reduce these releases over an approximate five (5) year period.

Enforcement of environmental regulations is carried out by the individual states which impose their own specific regulations which in some cases are even more stringent than those of the federal government. A case in point is the state of California where regulations are resulting in rapid actions on the part of corporations to comply or face harsh penalties. These actions include both a switch to alternative manufacturing materials and employment of new pollution control devices.

A new pollution control technology currently under development utilizes ultraviolet (UV) light to break down the volatile organic compounds (VOC's) contained in an

airstream. One pollution control equipment manufacturer has already employed this method in an installation in California (see Figure (1)). The process involves injecting ozone into a mixture of gaseous VOC's which have been radiated by UV light. In the presence of oxidants and UV light, the air/VOC mixture undergoes a series of photo-dissociation and radical oxidation reactions which destroy the VOC's. Despite this pollution control equipment's success in controlling a wide range of airborne VOC's, the extent of VOC reduction due to photolysis in the photolytic reactor section of the system is unknown. Our lack of information on the effectiveness of this photolytic reactor as shown in Figure (2) is due to proprietary information retained by the manufacturer, insufficient test data, and lack of an adequate model to predict its performance.

There have been some analytical and experimental studies reported in the literature on photochemical reactors (ie., Y. Harano and T. Matsura (1972)). However, these studies are generally directed towards simplified geometries which can be modeled analytically (ie., axial, elliptical, and columnar reactors) and which assume well-mixed conditions, low light absorption, uniform flow, and negligible diffusion. Experimentation has been directed towards determining the deviation between these highly simplified models and actual reactor performance in order to determine the effects of factors omitted. Few if any

TERR-AQUA ENVIRO SYSTEMS
AIR POLLUTION CONTROL TECHNOLOGY

TAES ULTRAVIOLET-OXIDATION CONTROL SYSTEMS have been designated as Best Available Control Technology (BACT) for Volatile Organic Compounds (VOC) and Reactive Organic Compounds (ROC).

The UV-Oxidation processes utilize a proprietary, on-site, self-regenerative system designed to meet the current EPA and most stringent local Air Quality District rules for capture and destruct efficiencies.

TAES AIR POLLUTION CONTROL FLOW DIAGRAM

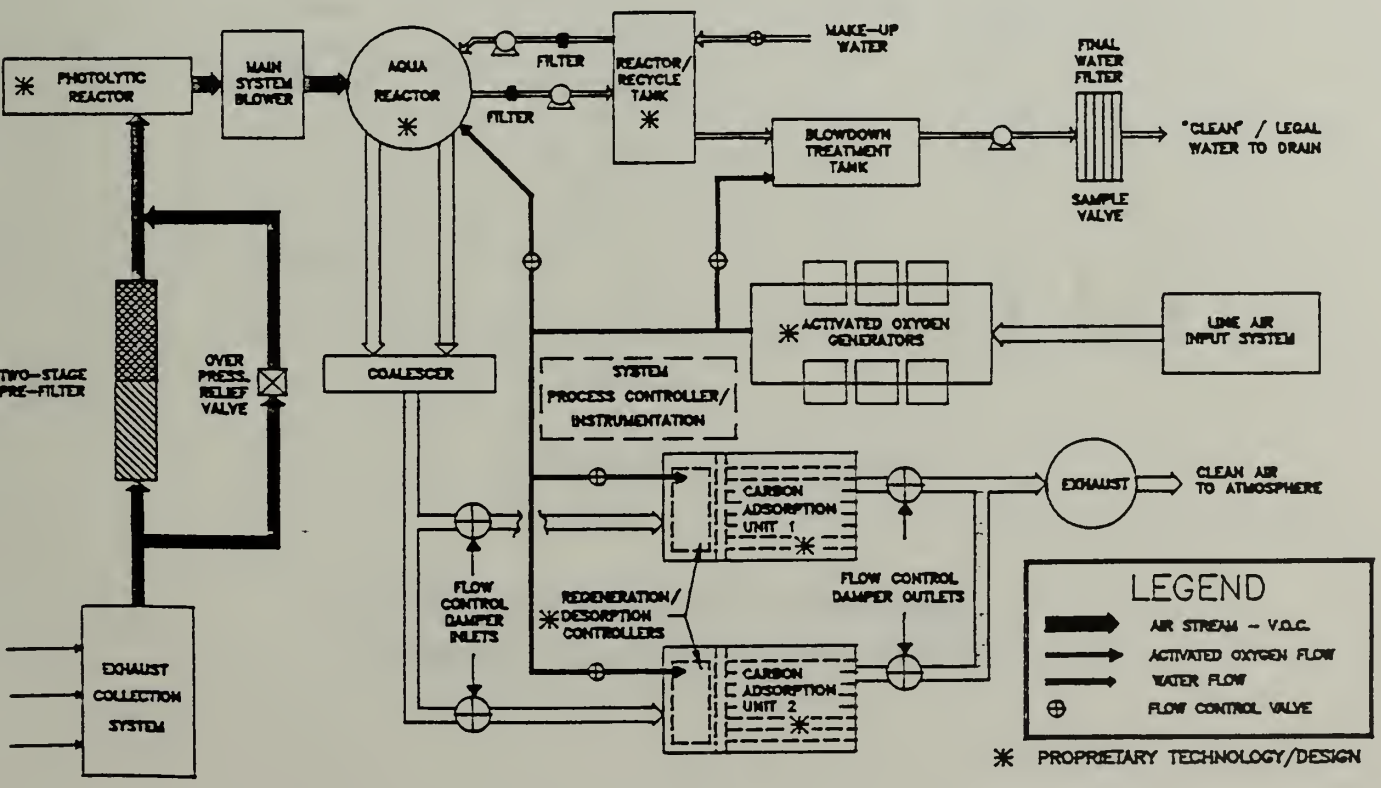

Figure (1) - VOC Pollution Control Device Schematic

(Terra-Aqua Environmental Systems (1992))

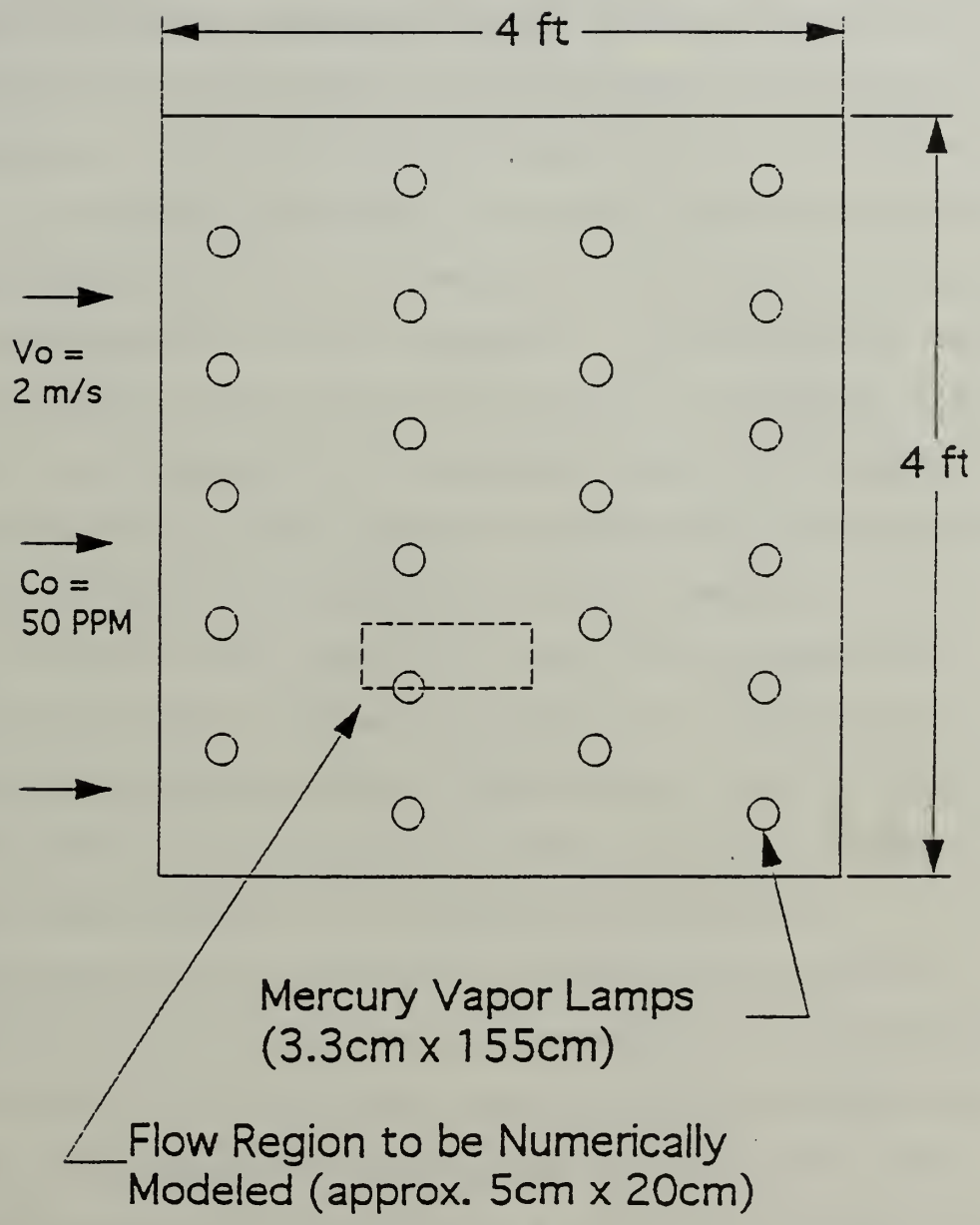

Figure (2) - VOC Pollution Control Device Photolytic Reactor

studies can be found in the literature which attempt to quantitatively model photochemical reactors of complex geometries and flow fields using numerical methods. This report provides a numerical model which can be used to quantitatively describe the photo-dissociation/radical oxidation of VOC's in the photolytic reactor of Figure (2).

A secondary but equally important objective for this analysis is to develop an analytical tool which can be used to optimize photo-reactor geometry. This numerical model, once verified with experimental data (in progress at Penn State) and expanded to incorporate additional reactants, can be utilized to predict optimum geometry for the photolytic reactor section of a pollution control device.

Finally, this model will assist the designer in determining when the use of a photolytic reactor in a pollution control device is appropriate. Since there are a multitude of VOC's which vary widely in their ability to react when exposed to UV light, cost effective implementation of a photolytic reactor may be highly dependant on the specific VOC's expected in an airstream. For example, the photolytic reactor may not provide any additional benefit in a pollution control device which treats specific emissions from a military or industrial painting operation. This numerical model may indicate when a significant cost savings is possible by omitting the photolytic reactor section and could also predict when the

photolytic reactor can function as the sole VOC reduction device in a pollution control system.

1.1 Literature Review

A review of literature on the subject of design and analysis of photochemical reactors shows that very little work has been accomplished in the area of numerical modeling.

Jacob, S. M. and Dranoff, J. S. (1969) conducted experiments on light distribution within an elliptical photoreactor and compared these results with some closed form solutions. They found that the closed form solutions are unable to accurately predict light intensity within an elliptical reactor. Additional studies by Jacob, S. M. and Dranoff, J. S. (1970) concluded that numerical means are required to accurately determine the light intensity distribution within a well-mixed elliptical photoreactor. While pointing out the necessity to use numerical methods in the analysis of photolytic reactors, neither of the above studies attempted to deal with reactors containing non-uniform flow fields and spatially varying reactant concentrations. In both studies only the case of simple elliptical geometry with laminar flow and well-mixed conditions was considered.

Work by Ragonese, F. P. and Williams, J. A. (1971) on the scale-up of a laboratory photoreactor model to meet

actual chemical production requirements outlines the difficulties in utilizing both dimensional analysis and empirical data. Although success has been achieved in this scale-up process, the methods used apply to simplified geometries with laminar flow and well-mixed conditions. This study points out the need for numerical modeling to enable a designer to scale photoreactors to meet production needs or to achieve sufficient pollutant reductions in a pollution control device.

The literature review provided by Harano, Y., and Matsura, T. (1972) describes the many difficulties involved in the design of photochemical reactors. They summarized that even for the simplified geometries which have been studied extensively to date including cylindrical, parallel plate, annular and elliptical reactors, the actual concentration gradients, light intensity distributions and flow conditions greatly influence overall reaction rates within the photoreactor.

All the literature reviewed on the subject of photolytic reactor design points to the need for numerical reactor modeling which incorporates both photochemical and fluid mechanics principles and the latest numerical solution techniques.

Chapter 2

PRELIMINARY MODELING ASSUMPTIONS

Due to the great difficulty in modeling the entire reactor under investigation including all possible chemical reactions, this model describes only the photo-dissociation/radical oxidation (photolysis) of formaldehyde in a rectangular flow field perpendicular to the axis of a single UV lamp as shown in Figure (2). Formaldehyde has been chosen for this model since its photochemistry has been studied, documented and verified. Although this model applies only to the photolysis of formaldehyde, it is general enough to incorporate the chemistry of other airborne components as well as combinations of other photochemically reactive solvents in the future. In addition, the principles required to expand this numerical analysis to additional materials and/or chemical reactions have been included in this report.

The following assumptions have been made to simplify the analysis:

A. Constant fluid properties (ie.,density, temperature, diffusion coefficient).

B. Negligible thermal effects (ie.,solution of energy conservation equations not required).

C. Two-dimensional flow field.

D. Weak absorbance of UV light (ie., light intensity is independent of formaldehyde concentration).

E. Photo-dissociation/radical oxidation of formaldehyde only. No other reactions between formaldehyde and other compounds are included except those required to complete the photo-dissociation/radical oxidation of formaldehyde.

F. Steady, time-averaged flow field (ie, no oscillation of vortex shedding in the wake region).

G. No wall losses (ie., chemical reactions which sometimes occur due to collisions of molecules into the reactor walls or the UV bulb itself).

H. No reflection of UV light from the reactor walls.

The above assumptions are considered to be reasonable ones for use in this initial numerical model. In the future, factors such as wall losses and reflection can be introduced into the numerical simulation to increase its accuracy.

Chapter 3

MASS CONSERVATION WITHIN THE PHOTOLYTIC REACTOR

Given the assumptions provided in Chapter 2, the differential equation which describes material concentration in the photolytic reactor can be written:

$$-v \circ \nabla C + D\nabla^2 C + \Omega = dC/dt \qquad [1]$$

where, C = concentration of formaldehyde (PPM).

v = flow velocity (with components v_x, v_y) (m/s).

D = formaldehyde diffusion coefficient (m^2/s).

Ω = generation of formaldehyde (PPM/s).

The first element of Equation [1], the convection term, involves the fluid mechanics of the reactor. It combines concentration changes along a given direction with the fluid velocity to result in a time rate of change in concentration.

The second term in the above equation is the diffusion term. It describes the time rate of change of concentration entering/leaving the control volume due to concentration gradients at the element surface. Note that this term is dependant on the second spatial derivative of C multiplied by a diffusion constant and is relatively small with respect to the velocities in the flow. To achieve the highest

accuracy possible for all possible concentration gradients and flow velocities, this term is included in the model.

The third term in this equation describes concentration changes due to the photolytic action of the UV bulb and other chemical reactions. For this model the "generation term" simplifies to the following:

$$\Omega = -KC \qquad [2]$$

where, K is the overall specific absorption rate constant (overall rate constant for the breakdown of formaldehyde by UV light).

The final term is the resultant time rate of change for the element which, when included yields a transient solution. Since the transient solution has practical value both in predicting the start-up concentrations within the reactor as well as in examining time varying inputs, the time dependant term has been included. In addition to the above benefits, a transient solution must be found in order to obtain convergence for the numerical solution technique used. This is required since it is difficult for the iterative numerical technique (Gauss-Seidel) to jump directly from zero time to an infinite solution (steady-state solution) without some intermediate steps in time.

For the case of a multi-component flow field which includes chemical reactions as well as photolytic reactions,

Equations [1] and [2] can be written:

$$-v \circ \nabla C_i + D_i \nabla^2 C_i + \Omega_i = dC_i/dt \qquad [3]$$

$$\Omega_i = -K_i C_i + \text{other reactions (see Appendix B)} \qquad [4]$$

Analysis of the multi-component case requires the solution of n simultaneous Equations ([3] and [4]) corresponding to the total number of reactants. Note that Appendix B contains numerous additional equations involving chemical and photochemical reactions between many possible airborne constituents. In order to simplify this analysis only the photolysis of formaldehyde will be considered (ie., no reactions between formaldehyde and other airborne constituents will be considered).

In the next chapter the determination of velocities required in the convection term of Equation [1] is discussed.

Chapter 4

FLUID MECHANICS PRINCIPLES

For the case of turbulent, viscous flow around the spherical bulbs shown in Figure (2), a complete solution of the Navier-Stokes equations is required to obtain accurate fluid velocities. Due to the difficulty in solving the complete Navier-Stokes equations, a commercially available computational fluid dynamics program has been employed to determine the velocities in a rectangular region around a single bulb. Figure(3) shows a standard K-ε method solution of the Navier-Stokes equations for flow of air around a circular cylinder generated by the FLUENT program. The shape of a 0.03m diameter circular cylinder in a 0.05m x 0.20m flow field has been approximated by a series of grid points (100 wide by 25 high). The program calculates x and y velocities at every grid point in the flow for input into the convection terms of Equation [1].

The following parameters were input to the FLUENT program (properties of air/solution parameters):

Properties of air only assumed (no air/form. mixture)
Length of domain (x direction, m)- 0.2
Height of domain (y direction, m)- 0.05
Diameter of Bulb (m)- 0.03
Grid size (x dir, y dir)- 100 x 25

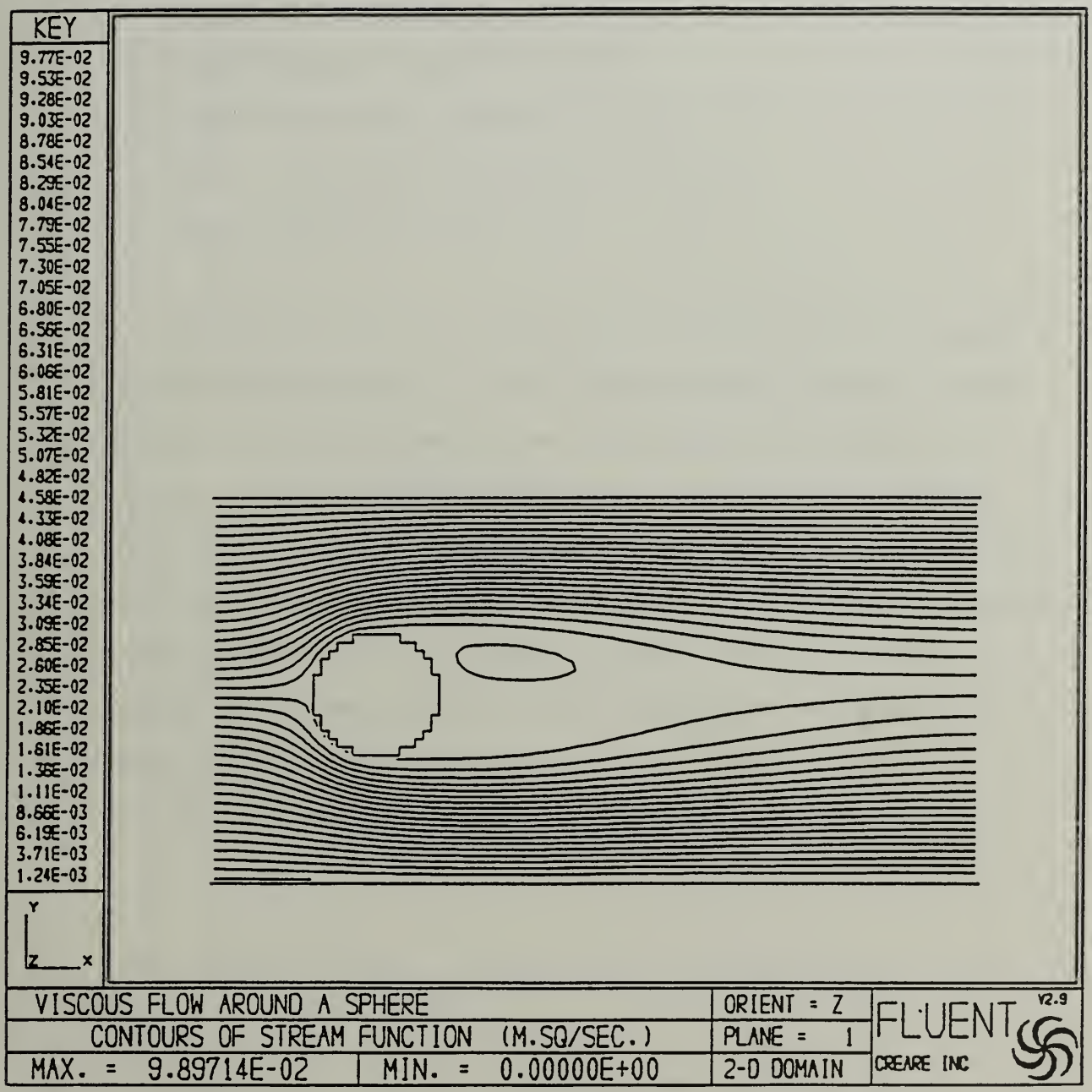

Figure (3) - FLUENT Generated Streamlines For Flow of Air Around a UV Lamp in a Uniform Flow Field

Reynolds Number, Re_D - 4,500

Inlet Temperature (°C)- 35

Inlet Pressure (Kpa)- 101.33

Inlet Density (kg/m^3)- 1.293

Inlet Viscosity (kg/m-s)- 1.72×10^{-5}

Inlet Turbulence Intensity (%)- 10.0

Inlet Velocity (m/s)- 2.0

Since it is beyond the scope of this report to examine the detailed accuracy of the FLUENT program output, these results will be assumed to be sufficiently accurate for the purpose of making design decisions. There are a variety of models and techniques which can be employed to increase and verify the accuracy of the flow analysis. However, since it is the purpose of this report to model the photolytic reactor in a fashion which well-exceeds the accuracy of simple plug flow models which can be found in the literature, the unmodified FLUENT output is used.

Chapter 5

CHEMICAL PRINCIPLES

The chemistry associated with the photolytic reactor under consideration here is much the same as that of atmospheric chemistry with the exception that energy is added with a mercury lamp which emits several discrete wavelengths (predominantly 253nm) versus sunlight which contains these and other wavelengths. The chemistry of the photolytic reactor can be broken down into two categories including photochemistry and free radical chemistry.

5.1 PHOTOCHEMISTRY

Photochemical processes initiated by UV radiation begin with the absorption of a photon by a molecule as follows:

$$A + h\upsilon \xrightarrow{K} A^* \qquad [5]$$

where, A^* is an exited A molecule and $h\upsilon$ is a photon of UV energy. Upon excitation the A^* molecule can undergo the following reactions:

Dissociation: $A^* \xrightarrow{K_1} B + C$ [6]

(A^* broken down into stable molecules by itself)

Direct Reaction: $A^* + B \xrightarrow{K_2} D + E$ [7]

(A^* combines with B to form two stable molecules)

Fluorescence: $A^* \xrightarrow{K_3} A + h\upsilon$ [8]

(A^* returns to orig. state after release of energy)

Collisional Deactivation: $A^* + B \xrightarrow{K_4} A + B + h\upsilon$ [9]

(A^* returns to orig. state after collision with B)

Each one of the above reactions has a probability of occurrence called a quantum yield, Φ_i. For example, a quantum yield of $\Phi_1 = 0.5$ implies that there is 50% chance that A^* molecules will undergo dissociation (Equation [6]) while there is a 50% chance A^* molecules will directly react, undergo fluorescence or deactivate from a collision. Since all the A^* molecules must undergo one of the above reactions:

$$\sum_{i=1}^{n} \Phi_i = 1 \qquad [10]$$

The production of A^* molecules is given by the following rate equation:

$$\frac{d[A^*]}{dt} = K[A] \qquad [11]$$

In Equation [5], since one A^* molecule consumes one molecule of A:

$$\frac{d[A]}{dt} = -K[A] \qquad [12]$$

The symbol K is the overall "specific absorption rate" constant (also given in Equation [2]) and [A*], [A] are the concentrations of A* and A, respectively. Note that the overall rate constant corresponds to all possible quantum yields for A*. By combining equations [5] through [9], the rate equations corresponding to the dissociation, direct reaction, fluorescence, and collisional deactivation reactions (termed the first order rate equations) can be written as follows:

$$\frac{d[A]}{dt} = -\Phi_1 K[A] = -K_1[A] \quad \text{(reduction in A due to dissociation)} \qquad [13]$$

$$\frac{d[A]}{dt} = -\Phi_2 K[A] = -K_2[A] \quad \text{(reduction in A due to direct reaction)} \qquad [14]$$

$$\frac{d[A]}{dt} = -\Phi_3 K[A] = -K_3[A] \quad \text{(reduction in A due to fluorescence)} \qquad [15]$$

$$\frac{d[A]}{dt} = -\Phi_4 K[A] = -K_4[A] \quad \text{(reduction in A due to collisional deactivation)} \qquad [16]$$

The quantities K_1 ($=\Phi_1 K$), K_2, K_3, and K_4 in Equations [13] through [16] are termed the first order rate constants. Note that multiplying both sides of Equation [10] by K results in $K_1 + K_2 + K_3 + K_4 = K$. Therefore, the overall reaction rate for the reduction of A is equal to the sum of the individual rates for reactions which can occur upon excitation of A molecules.

For the general case of atmospheric chemistry, the

first order rate constants can be determined through the following equation:

$$K_1 = \int_{\lambda_1}^{\lambda_2} \sigma(\lambda,T)\Phi_1(\lambda,T)\,I(\lambda)\,d\lambda \qquad [17]$$

$\sigma(\lambda,T)$ = absorption cross section of the A molecule at operating temp., pressure and UV wavelength (cm^2).

$\Phi_1(\lambda,T)$ = quantum yield or probability that molecule A will dissociate upon excitation (recalling that one molecule of A produces one molecule of A*) (K_2 would correspond to direct reaction rate).

$I(\lambda)d\lambda$ = irradiance of incident UV light (photons/cm^2-sec).

The above first order rate constant, K_1 corresponds to the rate at which molecule A will undergo dissociation (one of the four reactions mentioned above) when exposed to a broad spectrum of light energy in the atmosphere.

In order to calculate the first order rate constants for combinations of specific, discrete wavelengths the following approximation is utilized:

$$K_1 = \sum_{i=1}^{n} \sigma(\lambda_i,T)\Phi_1(\lambda_i,T)\,I(\lambda_i)\,\Delta\lambda \qquad [18]$$

The quantities σ and Φ_1 above are average values at λ_i. The quantity $I(\lambda_i)\Delta\lambda$ is sometimes expressed as $J(\lambda_i)$ (actinic flux) which results in the following:

$$K_1 = \sum_{i=1}^{n} \sigma(\lambda_i, T)\Phi_1(\lambda_i, T)J(\lambda_i) \qquad [19]$$

5.1.1 DETERMINATION OF FORMALDEHYDE PHOTOLYTIC RATE CONSTANTS

Formaldehyde participates in the following photolytic reactions ($\lambda \leq 300$nm):

$$HCHO + h\nu \xrightarrow{K_1} H + HCO \quad \text{(HCHO is formaldehyde)} \qquad [20]$$

$$\xrightarrow{K_2} H_2 + CO \qquad [21]$$

The wavelength of UV light utilized in this device is predominately λ = 253 nm. The bulb dimensions are as follows:

D (diameter) = 0.033 m

L (length) = 1.5536 m

P_{total} (total bulb power requirement) = 40 W (J/s)

$P_{visible}$ (bulb output in visible spectrum per manufacturer) = 40% P_{total}

P_{253} (bulb output at 253 nm) = 95% $P_{visible}$

As an example, the first order rate constant at λ=253nm (corresponding to the reaction of equation [20] above) is determined as follows:

$$E = hc/\lambda = \frac{6.6256\times10^{-34}\text{J-s/photon}(2.9979\times10^{8}\text{m/s})}{253\times10^{-9}\text{m}}$$

$$= 7.8509 \times 10^{-19}\text{J/photon}$$

$$A_{BULB} = \pi DL = \pi(33\text{mm})(1553.6\text{mm}) = 1611\ \text{cm}^2$$

$$P_{253} = 40\text{W}(40\%)(95\%) = 14.44\ \text{J/s}$$

$$J(\lambda=253\text{nm}) = \frac{P_{253}}{A_{BULB}(E)} = \frac{14.44\ \text{J/s}}{1611\ \text{cm}^2(7.8509 \times 10^{-19}\text{J/photon})}$$

$$= 1.1419 \times 10^{16}\ \text{photons/cm}^2\text{s}$$

σ(253nm,25C) = 3.79×10^{-21}cm^2/molecule (R. Atkinson, et al. (1992))

Φ_1(253nm,25C) = 0.3 (R. Atkinson, et al. (1992))

$$K_1 = \sigma(\lambda,T)\Phi_1(\lambda,T)J(\lambda)$$

$$= 3.79\times10^{-21}\text{cm}^2\text{/molecule}(0.3)(1.1419\times10^{16}\text{phot./cm}^2\text{s})$$

$$= 1.30 \times 10^{-5}\ (1/\text{s})$$

K = overall specific absorption rate (yields both reactions 1,2)

$$K = K_1 + K_2 = \sigma(\lambda,T)\Phi_1(\lambda,T)J(\lambda) + \sigma(\lambda,T)\Phi_2(\lambda,T)J(\lambda)$$

$$= \sigma(\lambda,T)(\Phi_1(\lambda,T)+\Phi_2(\lambda,T))J(\lambda)$$

Φ_2(253nm,25C) = 0.5 (R. Atkinson, et al. (1992))

$$K = (3.79\times10^{-21}\text{cm}^2/\text{molecule})(0.3+0.5) \times (1.1419\times10^{16}\text{photons/cm}^2\text{s})$$

$$= 3.47 \times 10^{-5}\ (1/s)$$ (yields both reactions 1,2 (Eqns [20],[21]))

5.1.2 LIGHT INTENSITY DISTRIBUTION THROUGHOUT THE REACTOR

The rate calculations above are based on the intensity at the bulb surface. This formulation is based on the Beer-Lambert law applied to weak absorbance conditions such as the atmosphere (Finlayson-Pitts, B. J., and Pitts, J. N., Jr. (1986)). Since the energy added via the bulb per unit area and corresponding rate constants vary indirectly with the radial distance from the bulb surface, Equation [2] must be modified as follows:

$$\Omega = -K(R/r)C \qquad [22]$$

where, r = radial distance from bulb centerline.

R = radius of bulb.

In addition, the light intensity in an actual photochemical reactor is also attenuated according to the well known Beer-Lambert law (Finlayson-Pitts, B. J., and

Pitts, J. N., Jr. (1986))which is written as follows:

$$I = Io \exp\{-\sigma NP\} \qquad [23]$$

where, Io = monochromatic source intensity(photons/cm^2-sec).
σ = absorption cross section (cm^2/molecule).
N = molecules/cm^3 (molar concentration).
P = path length from the source (cm).

For low concentrations and/or low absorbance, as is the case with this model, the effects of concentration on light intensity can be shown to be negligible. For this reactor:

$\sigma = 3.79 \times 10^{-21} cm^2$/molecule
N = 1.229×10^{15} molecules/cm^3 (equivalent to 50 PPM)
P = approx. 20 cm

Substituting into Equation [23] yields:

$$I = Io \exp\{-(3.79 \times 10^{-21} cm^2/\text{molecule}) \times (1.229 \times 10^{15} \text{ molecules}/cm^3)(20 \text{ cm})\}$$
$$= 0.99991 \, Io$$

In view of the above result it is clear that the weak absorbance assumption is a reasonable one.

In order to accurately model a multi-component air/VOC mixture where light absorbance must be considered, the following multi-reactant Beer-Lambert law is utilized:

$$I = Io \exp\{-[\sigma_1 N_1 + \sigma_2 N_2 + ...]L\} \qquad [24]$$

Using this relationship an intensity function, $I = f(x,y)$ can be determined using the actual concentration of materials in the reactor which are capable of absorbing light.

The specific photochemistry of reactants which could be considered in this model are contained in Appendix B. However, for the purpose of this initial model only the photolysis of formaldehyde is under consideration. Therefore, the intensity will be considered to be a function of the radial distance from the bulb surface only due to the weak absorbance of formaldehyde which was demonstrated above.

5.2 FREE RADICAL CHEMISTRY

As can be seen in Appendix B there are a multitude of reactions which can be included in this model as there are numerous materials normally contained in an airstream which are capable of undergoing photolysis and reacting with formaldehyde. However, due to the great complexity of including all these reactions, this initial model will be

only concerned with the removal of formaldehyde through photolysis alone. Therefore the "generation" term of Equation [1] will be that given by Equation [20] with no other reactions included.

Note that in making the above simplification, reactions with free radicals have been ignored. Therefore, the results of this investigation apply only to photolytic reactions. This analysis is a logical first step toward a more comprehensive analysis that will include free radical reactions. This analysis also provides valuable insight into the photolysis of formaldehyde in a non-uniform flow field.

Chapter 6

CLOSED FORM SOLUTION FOR SIMPLIFIED FLOW FIELD

In order to get a general idea of the size of the actual pollution control device required to reduce a given formaldehyde input concentration by a factor of two through photolysis, a simplified flow field model can be employed. Restating the mass conservation equation:

$$-v \circ \nabla C + D\nabla^2 C + \Omega = dC/dt \qquad [25]$$

The following simplifying assumptions will be made:

A. Two-dimensional, inviscid, steady flow.

   (v = velocity in x direction = constant,
   velocity in y direction = 0)

B. Constant radiance intensity throughout the reactor.

C. Formaldehyde photolysis only.

D. Diffusion negligible.

With these assumptions, the above equation simplifies to:

$$-v \circ \nabla C + \Omega = 0 \qquad [26]$$

Since the only reaction involves the photolysis of formaldehyde, substitution of Equation [2] into Equation

[26], performing the dot product and simplifying yields:

$$v \frac{dC}{dx} = -KC \qquad [27]$$

Rearranging terms and solving for C(x) yields:

$$\ln(C) - \ln(C_o) = -Kx/v \qquad [28]$$

$$\ln(C/C_o) = -Kx/v \qquad [29]$$

$$C/C_o = \exp\{-Kx/v\} \qquad [30]$$

The values assumed are:

$C/C_o = 0.5$
$K = 3.47 \times 10^{-5}$ (1/s) (as calculated)

$v = 5$ ft/s

Substituting in values and solving for x yields:

$X_{50} = 99,877$ ft = x corresponding to a 50% C reduction

= 18.9 miles

This result is a very pessimistic one which predicts poor performance for a reactor which relies on the photolysis of formaldehyde alone. However, in examining the general solution of the analytical model for different values of V and K, it appears that the analytical model can

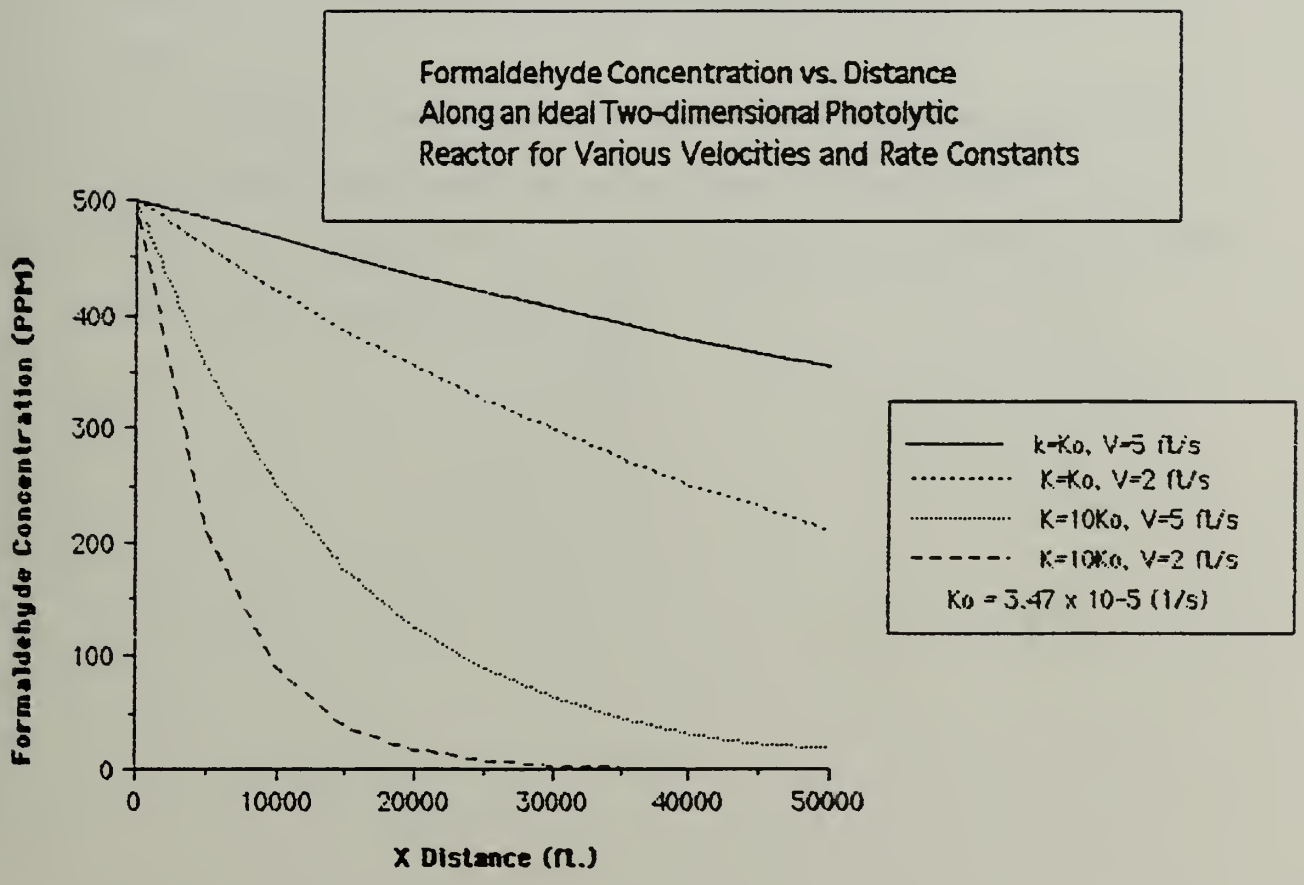

Figure (4) - Formaldehyde Concentrations in an Idealized Two-dimensional Columnar Photo-reactor

be significantly improved (see Figure(4)) by employing a higher intensity mercury lamp (increasing K) and/or by decreasing the flow velocity.

Increasing the intensity of the lamp is a viable option. There are currently bulbs available which are capable of over 1000 times the power of the mercury vapor lamps which are used in the photolytic reactor of Figure (2).

Since a decrease in velocity beyond some practical value will only lead to a decrease in the amount air treated, increasing the bulb intensity is clearly the best practical alternative.

Chapter 7

DEVELOPMENT OF THE NUMERICAL MODEL

The numerical photolytic reactor model under consideration predicts the concentrations in a rectangular area around a typical bulb in the reactor of Figure (2). Since very little reduction in formaldehyde is expected in a small 21.2 x 6.6 cm domain utilizing the actual rate constant calculated in chapter 5.1.1, the rate constant has been increased 10,000 times to an attainable 0.35 (1/s) to achieve some discernable results within two decimal places. Although this bulb intensity/reaction rate increase is presently impractical from a cost standpoint (very expensive bulbs are required) it greatly improves the analysis and interpretation of the numerical results for the small flow domain under consideration. The following data describe the parameters of the model:

L, length of the domain in x direction = .2121 m
M, number of nodes in the x direction = 100
h, size of increments in the x direction = 0.002143 m
H, length of the domain in the y direction = .0664 m
N, number of nodes in the y direction = 31
h, size of increments in the y direction = 0.002143 m
Uo, inlet velocity = 2.0 m/s (const. across entire area)

Co, inlet formaldehyde concentration = 50.0 PPM (")

Bulb diameter = .03 m

K, overall rate constant at bulb = .35 1/s

D, diffusion coefficient = 0.00002 m^2/s

ε, solution convergence criteria = 0.000001 PPM

(maximum difference between successive concentration calculations at each point at a given time)

Δt, time increment = 0.01 s

The computer model uses a finite difference technique in conjunction with a Gauss-Seidel iterative method to calculate the concentration field throughout the reactor at selected time intervals. The mass conservation equation is restated as follows:

$$-v \circ \nabla C + D\nabla^2 C + \Omega = dC/dt \qquad [31]$$

Since the convection terms dominate Equation [31], an upwind difference method has been incorporated into the above equation to improve the accuracy of the results. Simply stated, the upwind technique allows the concentration at any point i,j to be calculated based on points upwind since concentration changes are much more closely related to the fluid flow than they are to diffusion and photolytic

effects. Hence, differencing in the upwind direction is utilized for the convection terms. For the sake of simplicity, central differencing is used for the diffusion terms. The convection term of Equation [31] will now be developed in terms of finite differences.

The equation which follows, Equation [32], is an upwind difference expression which is valid when both the fluid velocity components, v_x and v_y are positive.

$$-v \circ \nabla C = -(v_x/h)(C_{i,j}-C_{i-1,j}) - (v_y/h)(C_{i,j}-C_{i,j-1}) \quad [32]$$

When both the fluid velocity components are negative:

$$-v \circ \nabla C = -(v_x/h)(C_{i+1,j}-C_{i,j}) - (v_y/h)(C_{i,j+1}-C_{i,j}) \quad [33]$$

An expression derived from Equations [32] and [33] above which will always yield an upwind difference for any combination of velocity component directions can be written as follows:

$$\begin{aligned} -v \circ \nabla C = -(1/2h)\{ & (|v_x| + v_x)(C_{i,j}-C_{i-1,j}) + \\ & (|v_y| + v_y)(C_{i,j}-C_{i,j-1}) + (v_x - |v_x|)(C_{i+1,j}-C_{i,j}) + \\ & (v_y - |v_y|)(C_{i,j+1}-C_{i,j})\} \end{aligned} \quad [34]$$

While the above equation may appear unnecessarily lengthy,

it greatly increases the speed of numerical calculations as a decision does not have to be made (FORTRAN IF statement) at each point in order to apply the correct equations based on the velocity component directions. Without condition statements in the calculation of the convective terms, much of the program can be vectorized to greatly reduce the computation time.

In terms of central differences, the diffusion term can be written:

$$D\nabla^2 C = (D/h^2)\{C_{i+1,j} + C_{i-1,j} - 4C_{i,j} + C_{i,j+1} + C_{i,j-1}\} \quad [35]$$

The remaining terms are:

$$\Omega = -KC_{i,j} \quad [36]$$

$$dC/dt = (1/\Delta t)(C_{i,j}^{n} - C_{i,j}^{n-1}) \quad [37]$$

The superscripts n and n-1 above refer to the present value and the value at the previous time, respectively. It is important to note that a backward difference scheme has been employed for the time dependant solution of the governing equation. Although all terms on the left side of the governing equation (Eqn. [31]) have been developed using concentration values at the present time, the superscript n

has been omitted for clarity. The backward difference method results in an implicit set of equations which can be solved by the Gauss-Seidel iterative method to find the concentration at each point in the reactor at a particular point (iteration) in time, n. This method may seem cumbersome in comparison to the forward difference method which can explicitly calculate the concentrations at a future point in time without iteration. However, the backward difference method has higher stability which allows a much larger time step to be used.

Substituting Equations [33] through [37] into Equation [28] and solving for $C_{i,j}$ yields the following iterative equation:

$$C_{i,j}^{k+1} = \left\{\frac{1}{|v_x| + |v_y| + (4D/h) + hK + (h/\Delta t)}\right\} \left\{ (1/2)\{ (|v_x| + v_x) C_{i-1,j}^{k+1} + (|v_y| + v_y) C_{i,j-1}^{k+1} + (|v_x| - v_x) C_{i+1,j}^{k} + (|v_y| - v_y) C_{i,j+1}^{k}\} + (D/h)\{ C_{i+1,j}^{k} + C_{i-1,j}^{k+1} + C_{i,j+1}^{k} + C_{i,j-1}^{k+1}\} + (h/\Delta t) C_{i,j}^{n-1}\right\} \quad [38]$$

The superscripts k and k+1 in equation [38] represent concentration values calculated at the past and present iterations, respectively. Note that the $C_{i-1,j}$ and $C_{i,j-1}$ terms have the superscript k+1 whereas the $C_{i+1,j}$ and $C_{i,j+1}$ terms have the superscript k. This is due the iterative "search pattern" which sweeps from j=1 to

N (y=0 to y=H) for each i until i=M (x=L) is reached. This particular sweep pattern in conjunction with the Gauss-Seidel method makes use of the latest values (k+1) for $C_{i-1,j}$ and $C_{i,j-1}$ in calculating the updated $C_{i,j}^{k+1}$ value.

The boundary conditions of the flow domain are set as follows:

A. Inlet - C_i = const. = Co $(i=1; 1 \leq j \geq 25)$ [39]

B. Top and bottom surfaces - dC/dy = 0 (symmetry) or,

$$C_{i,j+1} = C_{i,j-1} \quad (1 \leq i \geq 100; j=1,25) \qquad [40]$$

C. At bulb - dC/dx, dC/dy = 0 (solid boundary) or,

$$C_{i+1,j} = C_{i-1,j} \quad \text{(see program, Appendix A)} \qquad [41]$$

$$C_{i,j+1} = C_{i,j-1} \quad \text{(see program, Appendix A)} \qquad [42]$$

D. Exit - dC/dx = 0 (minimal change at exit) or,

$$C_{i,j} = C_{i-1,j} \quad (i=100; 1 \leq j \geq 25) \qquad [43]$$

The computer program included in Appendix A uses Equation [38] (including the relationships of Equations [39] through [43] when required) to calculate and update new concentration values at all grid points in the domain per each iteration. The iterations converge to the solution for a given time step when the present and previous concentration values for each point in the entire domain differ by less than an epsilon value (i.e., $\left| C_{i,j}^{k+1} - C_{i,j}^{k} \right| \leq \varepsilon$ for all points in the domain).

Figure (5) is a graphical representation of the program

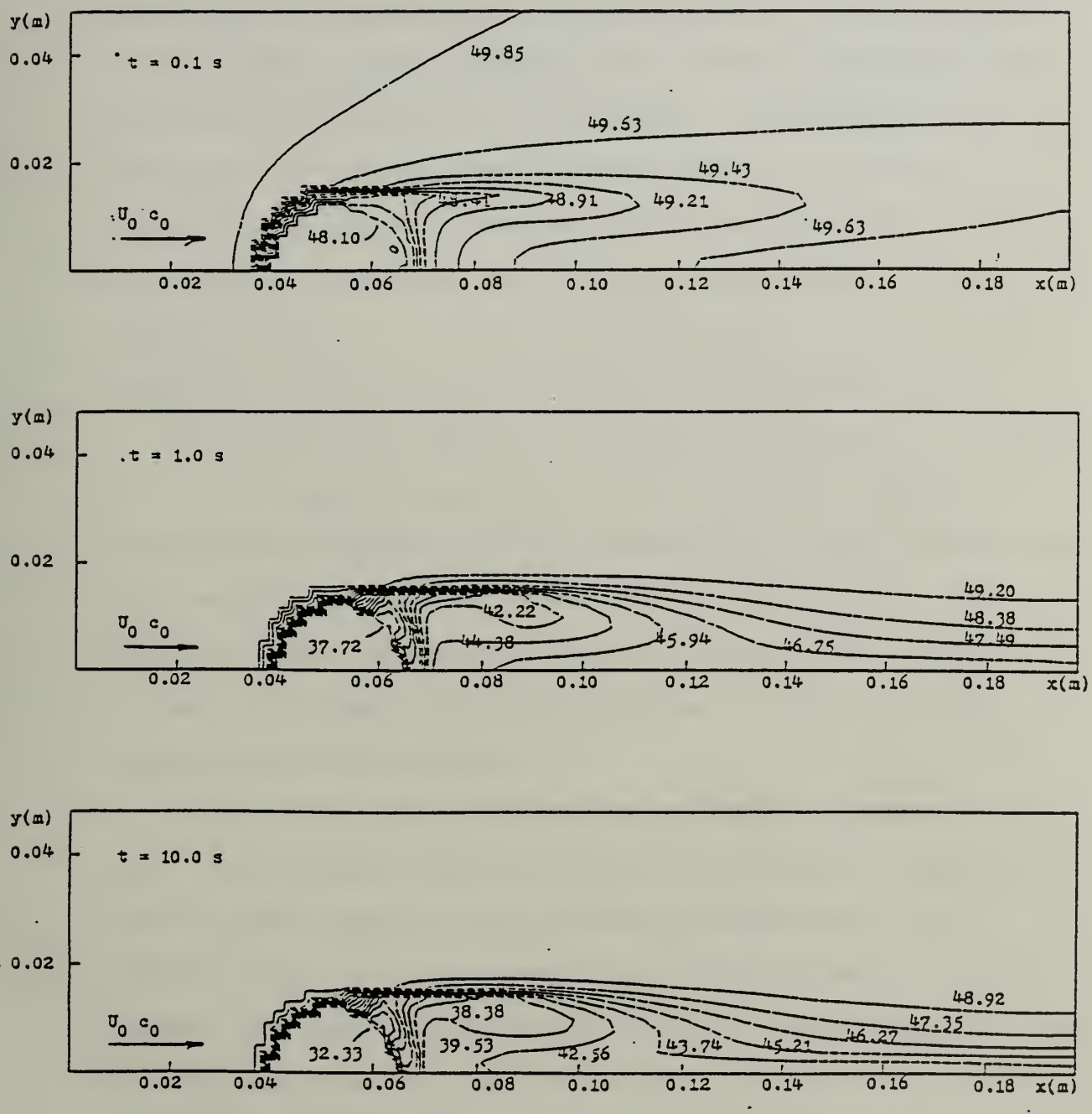

Figure (5) - Formaldehyde Concentrations Within the Numerical Photo-reactor Model

output for selected values of time. The solution at t = 10 sec is considered to be a steady state solution. This was determined by comparing the solutions at t = 10 sec and t = 100 sec which did not differ to two decimal places for the vast majority of points in the domain. In addition, to ensure that a time-accurate, steady state solution was obtained, the computer program was run at Δt=0.005 s (half the original time step) out to a 10 sec solution. The results of this run did not differ from the original 10 sec solution to over 4 decimal places for the entire domain.

The numerical concentration predictions for the "start-up" of the reactor make sense from a practical standpoint. The smallest concentrations are seen at the bulb surface and wake regions due to the low fluid velocities there. In addition, these regions of lesser concentration migrate further downstream with increased time as they are swept into the bulb wake region.

The steady state isopleths also appear reasonable in form. As expected, these concentration contours generally form the same shape as the streamlines depicted in the FLUENT output due to the dominance of the convection terms. However, the isopleth shapes differ from the streamlines due to diffusive transport and photolysis. In the next chapter it will be shown by comparison with the simplified flowfield model that the magnitude of formaldehyde reductions shown in Figure (5) are reasonable predictions.

Chapter 8

ANALYSIS OF RESULTS

In order to obtain a general performance check on the numerical solution, the simplified flow model developed in Chapter 5 can be employed by inputting the numerical model parameters discussed in Chapter 7 into Equation [30] as follows:

$Co = 50$ (PPM)

$K = 0.35$ (1/s)

$v = 2.0$ (m/s)

$x = 0.2121$ (m)

Substituting values into equation [30] yields:

$$C = Co \exp\{-Kx/v\}$$
$$= 50.0\text{PPM} \exp\{-0.35s^{-1}(0.2121\text{m})/2.0\text{m/s}\}$$
$$= 48.17 \text{ PPM}$$

The above result compares favorably with the 49.37 PPM average steady state concentration leaving the numerical reactor model which was found through a mass average taken across the exit as follows:

$$C_{exit,avg.} = \Sigma v_i C_i / \Sigma v_i \qquad [45]$$

In the next paragraph the analytical and numerical results are compared in terms of destruction efficiencies.

An additional comparison between the numerical and simplified flow field models is obtained by introducing parameters which define the destructive efficiency of the photolytic reactor. Since it is the objective of the reactor model to eliminate formaldehyde, the efficiency of the entire reactor section can be defined as follows:

$$E = 1 - (C_{exit,avg.}/C_{inlet}) \qquad [46]$$

In addition to the above equation it is also useful to define an efficiency which is based on the bulb height alone. This term is defined as follows:

$$E_B = 1 - (C_{exit,avg.}/C_{inlet}) \qquad [47]$$

Equation [47] calculates an efficiency based on a collimated region with a height equal to the radius of the bulb. In Equation [47] the term $C_{exit,avg.}/C_{inlet}$ is taken from the centerline of the reactor up to the bulb radius. Table-1 compares the efficiency of the steady state numerical simulation of the photolytic reactor section with that of the simplified flow field model.

	Numerical Model (PPM)	Simplified flow Field Model (PPM)
C (average across entire reactor section)	49.37	48.17
C (average up to bulb radius)	47.37	48.17
E (based on entire reactor cross section)	1.26%	3.64%
E_B (based on bulb width)	5.26%	3.64%

Table-1 Comparison of Numerical and Simplified Flow Models

For this set of conditions it appears that the simplified flow field model is more efficient than the numerical reactor model when the efficiency is based on the entire reactor cross section. However, in examining the efficiencies based on the bulb cross section, the numerical reactor model which incorporates the actual flow conditions is superior to the simplified flow field model in its ability to destroy the formaldehyde. This result leads one to believe that a reactor containing a combination of bulbs which allows the incoming flow to "see" bulbs across the entire reactor area will out-perform the idealized columnar

reactor.

The advantage of using multiple bulbs is best illustrated by considering a single bulb reactor of infinite height. In such a reactor the UV bulb would have little effect on the VOC concentrations in the far stream. As shown in Figure (5), the bulb has the most influence (concentration reductions) in a columnar region which is one to two bulb diameters in height. In other words, the incoming flow which exists outside this columnar region tends to escape untreated. Therefore, an arrangement of bulbs which guarantees that all the incoming flow will encounter a bulb cross section (ie., a staggered stack of bulbs/columnar regions in parallel with no "escape" regions in between) would have a destructive efficiency of no less than that given by Equation [47].

In addition to the general advantages of a parallel bulb arrangement as described above, large-scale destructive efficiency improvements for both series and parallel arrangements are predicted by drawing an analogy between particle collection and VOC destruction in a photolytic reactor. For such an analogy the multi-bulb efficiency is given by the following (Heinsohn, 1991):

$$E_{overall} = 1 - (1 - E_B)^N \qquad [48]$$

where, N is the number of bulbs.

A twenty-five (N = 25) bulb arrangement with single bulb efficiencies as given by Equation [47] (E_B = 5.26% in this case) would have an overall destructive efficiency as follows:

$$E_{overall} = 1 - (1 - E_B)^N = 1 - (1 - 0.0526)^{25}$$
$$= 74.1\%$$

Although the particle collector/photolytic reactor analogy drawn here predicts very optimistic results, it will be necessary to confirm this relationship with a multi-bulb numerical model and/or experimental testing to achieve a high degree of confidence.

Chapter 9

CONCLUSIONS

This analysis clearly demonstrates the influence of actual flow conditions on the effectiveness of a photolytic reactor. Despite the simplifying (but reasonable) assumptions made in development of the numerical model, it provides valuable insight into the inner workings of the actual photolytic reactor. The graphical results of Figure (5) show that the velocity gradients, recirculation and mixing which occur within the reactor contribute greatly to the overall reduction of reactants. Since recirculation and mixing greatly increase the reduction of formaldehyde in the reactor, one would expect that unsteadiness in the flow field would tend to improve the results (noting that unsteadiness exists in the actual flow field under consideration due to vortex shedding). In addition, one would expect that an optimum Reynolds number, R_e could be found (input velocity) which would maximize the benefits of mixing while still providing an acceptable level of air treatment. Therefore, future numerical optimization studies should include both an unsteady flow field analysis and a comparison of results for different Reynolds numbers.

Although the simplified flow field model developed in this report can be used to obtain a rough estimate of reactor performance, it is unable to predict the effects of

the actual flow field which were found to be of great importance through an analysis of the numerical model results. This fact reinforces the need to use a numerical model in the optimization of a photolytic reactor design.

Comparison of efficiencies between the simplified flow field and numerical models provides some highly instructive results. Surprisingly, though the light intensity in the numerical model is more than five times less than that of the simplified flow field model for a large portion of the domain (due to the radial light attenuation from the lamp surface), the numerical model provides a comparable formaldehyde reduction performance when the efficiency is based on the entire reactor cross section. In addition, it appears that increasing the number of bulbs will greatly improve overall reactor effectiveness as indicated by a comparison of efficiencies based on the bulb width. Due to the optimistic results obtained in comparing the numerical and simplified flow field models, the next logical step for future research in this area should include the modeling of larger flow domains which contain a larger quantity of bulbs.

This undertaking also showed that additional factors can readily be taken into consideration in future reactor modeling. The computer program of Appendix A and techniques described in this analysis can be extended to include additional chemical reactions and other factors such as

Beer-Lambert light attenuation by reactants which will result in a numerical model of much greater accuracy. Although this work is of limited scope for practical reasons, expansion of this analysis including the use of a high-speed supercomputer could achieve an accurate numerical simulation of the entire photolytic reactor of Figure (2).

Despite the good correlation between the numerical and simplified flow field models developed in this report, a high degree of confidence can only be achieved through laboratory experiments whose results can be compared to the numerical ones. Therefore, future work should include experimental verification. This will be especially important when additional reactants and other factors are introduced. In the future, the benefits of a closed form solution as experienced in this development (simplified flow field model) will not be possible when modeling a highly complex reactor.

REFERENCES

Anatasi, C. Gladstone, R., and Sanderson, M.G., "Chemical Amplifiers for Detection of Peroxyl Radicals in the Atmosphere", Environmental Science and Technology, vol. 27, no. 3, 1993.

Atkinson, R., Baulch, D. L., Cox, R. A., Hampson, R. F., Jr., Kerr, J. A., and Troe, J., "Evaluated Kinetic and Photochemical Data for Atmospheric Chemistry," Journal of Physical and Chemical Reference Data, Vol. 21, No. 6, Nov/Dec, 1992.

Atkinson, R., Baulch, D. L., Cox, R. A., Hampson, R. F., Jr., Kerr, J. A., and Troe, J., "Evaluated Kinetic and Photochemical Data for Atmospheric Chemistry," Journal of Physical and Chemical Reference Data, Vol. 18, No. 881, 1989.

Atkinson, R., Baulch, D. L., Cox, R. A., Hampson, R. F., Jr., Kerr, J. A., and Troe, J., "Evaluated Kinetic and Photochemical Data for Atmospheric Chemistry," Journal of Physical and Chemical Reference Data, Vol. 13, No. 1259, 1984.

Calvert, J.G., and Pitts, J.N., "Photochemistry", John Wiley

and Sons Inc., New York, 1967.

Demore, W.B., et al., "Chemical Kinetics and Photochemical Data for use in Stratospheric Modeling", evaluation number 9, NASA, January, 1990.

Finlayson-Pitts, B.J., and Pitts, J.N. Jr, "Atmospheric Chemistry: Fundamentals and Experimental Techniques", Wiley-Interscience, New York, 1986.

Graham, R.A., and Johnston, H.S., "The Photochemistry of NO3 and the Kinetics of the N2O5-O3 System", Journal of Physical Chemistry, vol. 82, pgs. 254-258, 1978.

Harano, Y., and Matsura, T., "Problems in Designing Photochemical Reactors", International Chemical Engineering, Vol. 12, No. 1, pgs. 131-143, January 1972.

Heichlen, J., "Atmospheric Chemistry", Academic Press, New York, 1976.

Heinsohn, R.J., "Industrial Ventilation, Engineering Principles", Wiley, New York, 1991.

Jacob, S. M. and Dranoff, J. S., "Light Intensity Profiles in an Elliptical Photoreactor", International Chemical

Engineering, Vol. 15, No. 1, pgs. 141-144, January 1969.

Jacob, S. M. and Dranoff, J. S., "Light Intensity Profiles in a Perfectly Mixed Photoreactor", International Chemical Engineering, Vol. 16, No. 3, pgs. 359-363, May 1970

Johnson, H.S., Page, M., and Yao, F., "Oxygen Absorption Cross-section in the Herzberg Continum Between 206 and 327K", Journal of Geophysical Resources, vol. 89, pgs. 11661-11665, 1984.

Ragonese, F. P. and Williams, J. A., "Application of Empirical Rate Expressions and Conservation Equations to Photoreactor Design", International Chemical Engineering, Vol. 17, No. 6, pgs. 1352-1359, November 1971

Seinfeld, J.H., "Atmospheric Chemistry and Physics of Air Pollution," Wiley, New York, 1986.

Stockwell, W.R., and Calvert, J.G., "The Ultraviolet Absorption Spectrum of Gaseous HONO and N2O3", Journal of Photochemistry, vol. 8, pgs. 193-208, 1978.

Terr-Aqua Environmental Systems, Glendale, CA, Product Literature, 1992.

Appendix A

COMPUTER PROGRAM

```
C SET UP VARIABLES
      IMPLICIT DOUBLE PRECISION (A-H,O-Z)
      DIMENSION VX(100,33),VY(100,33),FMC(100,33),FMCOLD(100,33)
      X0=4.286
      Y0=0.0
      R0=1.50
      M=100
      N=31
      H=0.002143
      EPSI=0.0000001
      DT=0.01
      ITER=1
      ITERT=1
      ITEST=1
      ITERMAX=200
      ITERTMAX=10
C ENTER FORMALDEHYDE CONSTANTS
      FMRC0=0.35
      FMD=0.00002
      FMC0=50.0
C READ IN FLUENT GENERATED VELOCITIES
      OPEN(UNIT=5,FILE='SINGLEBULBLIS.DAT',STATUS='OLD')
      K=1
      KK=1
      KKK=10
    2 READ(5,5) ((VX(I,33-J),I=KK,KKK),J=1,N)
      K=K+1
      KKK=K*10
      KK=(K*10)-9
      IF(K.LE.10) GO TO 2
      K=1
      KK=1
      KKK=10
    3 READ(5,5) ((VY(I,33-J),I=KK,KKK),J=1,N)
      K=K+1
      KKK=K*10
      KK=(K*10)-9
      IF(K.LE.10) GO TO 3
      CLOSE(UNIT=5)
    5 FORMAT(5X,10E12.4)
C SET THE INITIAL FORMALDEHYDE CONCENTRATIONS
      DO 10 I=1,M
      DO 10 J=1,N+2
      FMC(I,J)=FMC0
      FMCOLD(I,J)=FMC0
   10 CONTINUE
C CALCULATE THE CONCENTRATIONS AT EACH POINT USING GAUSS-SEIDEL METHOD
   15 DO 50 I=2,M-1
      DO 50 J=2,N+1
      TEMP=FMC(I,J)
C  CALCULATE THE PHOTOLYTIC RATE CONSTANT
      FMRC=FMRC0*R0/((100.*H*(I-1)-X0)**2.+(100.*H*(J-2))**2.+
     $0.00000000001)**0.5
```

```
C APPLY BOUNDARY CONDITIONS (BC'S) AT THE BULB (J=2,I=14;J=4,I=15;
C                                              J=6,I=16,J=7,I=17,J=8,I=19)
      IF(((J.EQ.2).AND.(I.EQ.14)).OR.((J.EQ.4).AND.(I.EQ.15)).OR.
     $((J.EQ.6).AND.(I.EQ.16)).OR.((J.EQ.7).AND.(I.EQ.17)).OR.
     $((J.EQ.8).AND.(I.EQ.19)))
     $FMC(I,J)=(1/(4.*FMD/H**2.+FMRC+1./DT))*
     $((FMD/H**2.)*(2.*FMC(I-1,J)+2.*FMC(I,J+1))+FMCOLD(I,J)/DT)
C APPLY BOUNDARY CONDITIONS (BC'S) AT THE BULB (J=2,I=28;J=4,I=27;
C                                              J=6,I=26,J=7,I=25,J=8,I=23)
      IF(((J.EQ.2).AND.(I.EQ.28)).OR.((J.EQ.4).AND.(I.EQ.27)).OR.
     $((J.EQ.6).AND.(I.EQ.26)).OR.((J.EQ.7).AND.(I.EQ.25)).OR.
     $((J.EQ.8).AND.(I.EQ.23)))
     $FMC(I,J)=(1/(4.*FMD/H**2.+FMRC+1./DT))*
     $((FMD/H**2.)*(2.*FMC(I+1,J)+2.*FMC(I,J+1))+FMCOLD(I,J)/DT)
C  SKIP AREAS INSIDE THE BULB
      IF((((J.GE.2).AND.(J.LE.3)).AND.((I.GE.15).AND.(I.LE.27))).OR.
     $(((J.GE.4).AND.(J.LE.5)).AND.((I.GE.16).AND.(I.LE.26))).OR.
     $((J.EQ.6).AND.((I.GE.17).AND.(I.LE.25))).OR.((J.EQ.7).AND.
     $((I.GE.18).AND.(I.LE.24))).OR.((J.EQ.8).AND.((I.GE.20).AND.
     $(I.LE.22)))) GO TO 50
C  CALCULATION FOR GENERAL POINTS
      IF((J.GE.9).OR.
     $(((I.LE.13).OR.(I.GE.29)).AND.(J.EQ.2)).OR.
     $(((I.LE.14).OR.(I.GE.28)).AND.((J.GE.3).AND.(J.LE.4))).OR.
     $(((I.LE.15).OR.(I.GE.27)).AND.((J.GE.5).AND.(J.LE.6))).OR.
     $(((I.LE.16).OR.(I.GE.26)).AND.(J.EQ.7)).OR.
     $(((I.LE.18).OR.(I.GE.24)).AND.(J.EQ.8)))
     $FMC(I,J)=(1/((ABS(Vx(I,J))+ABS(VY(I,J))+4.*FMD/H)/H+FMRC+1./DT))*
     $(((ABS(VX(I,J))+VX(I,J))*FMC(I-1,J)+(ABS(VX(I,J))-VX(I,J))*
     $FMC(I+1,J)+(ABS(VY(I,J))+VY(I,J))*FMC(I,J-1)+
     $(ABS(VY(I,J))-VY(I,J))*FMC(I,J+1))/(2.*H)+(FMD/H**2.)*
     $(FMC(I-1,J)+FMC(I+1,J)+FMC(I,J-1)+FMC(I,J+1))+FMCOLD(I,J)/DT)
      IF(ABS(FMC(I,J)-TEMP).GT.EPSI) ITEST=ITEST*0.
   50 CONTINUE
C ASSIGN VALUES REQUIRED DUE TO BOUNDARY CONDITIONS
      DO 52 I=2,M-1
      FMC(I,1)=FMC(I,3)
      FMC(I,33)=FMC(I,31)
   52 CONTINUE
      FMC(20,8)=FMC(20,10)
      FMC(21,8)=FMC(21,10)
      FMC(22,8)=FMC(22,10)
      FMC(18,7)=FMC(18,9)
      FMC(24,7)=FMC(24,9)
      FMC(16,5)=FMC(14,5)
      FMC(26,5)=FMC(28,5)
      FMC(15,3)=FMC(13,3)
      FMC(27,3)=FMC(29,3)
C  APPLY BC'S AT END (DC/DX=0)
      DO 55 J=1,N+2
   55 FMC(M,J)=FMC(M-1,J)
      IF(ITER.GE.ITERMAX) GO TO 60
      IF(ITEST.EQ.1) GO TO 60
```

```
      ITER=ITER+1
      ITEST=1
      GO TO 15
   60 IF(ITERT.EQ.ITERTMAX) GO TO 64
      DO 62 I=2,M
      DO 62 J=2,N+1
   62 FMCOLD(I,J)=FMC(I,J)
      ITER=1
      ITERT=ITERT+1
      ITEST=1
      GO TO 15
C WRITE OUT RESULTS
   64 OPEN(UNIT=6,FILE='NEWSINGLE.OUT',STATUS='NEW')
      OPEN(UNIT=8,FILE='SINGLEPLOT.DAT',STATUS='NEW')
      DO 100 I=15,27
      DO 100 J=2,8
C  ASSIGN VALUES TO ACHIEVE A DECENT CONTOUR PLOT USING GNUPLOT
  100 IF((((J.GE.2).AND.(J.LE.3)).AND.((I.GE.15).AND.(I.LE.27))).OR.
     $(((J.GE.4).AND.(J.LE.5)).AND.((I.GE.16).AND.(I.LE.26))).OR.
     $((J.EQ.6).AND.((I.GE.17).AND.(I.LE.25))).OR.((J.EQ.7).AND.
     $((I.GE.18).AND.(I.LE.24))).OR.((J.EQ.8).AND.((I.GE.20).AND.
     $(I.LE.22)))) FMC(I,J)=30.
      SUM=0.
C  CALCULATE EXIT AVERAGES
      SUMD=0.
      SUM1=0.
      SUM1D=0.
      DO 80 J=2,N+1
      SUMD=SUMD+VX(100,J)
   80 SUM=SUM+FMC(100,J)*VX(100,J)
      SUM=SUM/SUMD
      DO 81 J=2,9
      SUM1D=SUM1D+VX(100,J)
   81 SUM1=SUM1+FMC(100,J)*VX(100,J)
      SUM1=SUM1/SUM1D
      K=1
      KK=1
      KKK=10
      WRITE(6,71) ITER,ITERT,SUM,SUM1,DT,EPSI
   65 WRITE(6,70) ((FMC(I,33-J),I=KK,KKK),J=1,N)
      K=K+1
      KKK=K*10
      KK=(K*10)-9
      IF(K.LE.10) GO TO 65
      DO 67, J=2,N+1
      DO 66, I=1,M
   66 WRITE(8,68) FMC(I,J)
      WRITE(8,69)
   67 CONTINUE
   68 FORMAT(F12.8)
   69 FORMAT(1X)
   70 FORMAT(10F12.8)
   71 FORMAT(2I6,4E12.4)
      STOP
      END
```

Appendix B

ATMOSPHERIC CHEMISTRY

WELL-MIXED MODEL OF PHOTO-OXIDATION AND RADICAL OXIDATION PROCESSES

Contents:

Note:

R represents a reaction; P represents a photolytic reaction; KR represents a rate constant; KP represents a photolytic rate constant.

Photolysis:

λ for the laser experiment will be 337 nm
input file "RATE"
$E_{Photon}=590*10^{-21}$ J/Photon

Actinic Flux=$20*10^{15}$ Photons/(cm^2*s)

$HCHO+h\nu \rightarrow H^*+HCO^*$	λ<300nm	4.08E-5 s^{-1}	[P1A]	Atkinson
$HCHO+h\nu \rightarrow CO+H_2$	λ≥300nm	2.97E-4 s^{-1}	[P1B]	Atkinson
$CH_3OH+h\nu \rightarrow$ negligible		0	[P2]	-----
$O_3+h\nu \rightarrow O(^1D)+O_2$	λ≤411nm	0	[P3A]	Atkinson
$O_3+h\nu \rightarrow O(^3P)+O_2$	λ<1180nm	0, (Φ = 0)	[P3B]	Atkinson
$O_2+h\nu \rightarrow O(^1D)+O(^3P)$	λ<175nm	0	[P4A]	Atkinson
$O_2+h\nu \rightarrow O(^3P)+O(^3P)$	λ<242nm	0	[P4B]	Johnson/ Atkinson
$O_2+h\nu \rightarrow O(^1D)+O(^1D)$	λ<137nm	0	[P4C]	Johnson/ Atkinson
$H_2O_2+h\nu \rightarrow OH^*+OH^*$	λ<557nm	1.40E-5 s-1	[P5A]	Atkinson
$H_2O_2+h\nu \rightarrow H_2O+O(^1D)$	λ<359nm	0, (Φ = 0)	[P5B]	Atkinson
$H_2O_2+h\nu \rightarrow H^*+HO_2^*$	λ<324nm	0, (Φ = 0)	[P5C]	Atkinson
$H_2O_2+h\nu \rightarrow 2H^*+O_2$	λ<213nm	0	[P5D]	Atkinson
$NO_2+h\nu \rightarrow NO+O(^1D)$	λ≤244nm	0	[P6A]	Atkinson
$NO_2+h\nu \rightarrow NO+O(^3P)$	λ<398nm	7.08E-3 s^{-1}	[P6B]	Atkinson
$H_2O+h\nu \rightarrow H_2+O(^3P)$	λ<243nm	0	[P7A]	Atkinson
$H_2O+h\nu \rightarrow H^*+OH^*$	λ<239nm	0	[P7B]	Atkinson
$H_2O+h\nu \rightarrow H_2+O(^1D)$	λ<176nm	0	[P7C]	Atkinson
$CO_2+h\nu \rightarrow CO+O(^1D)$		negligible		
$CO_2+h\nu \rightarrow CO+O(^3P)$		negligible		
$HONO+h\nu \rightarrow NO+OH^*$	λ<591nm	3.23E-3s-1	[P50A]	Atkinson
$HONO+h\nu \rightarrow H^*+NO_2$	λ<367nm	0, (Φ = 0)	[P50B]	Atkinson
$HONO+h\nu \rightarrow HNO^*+O(^3P)$	λ<283nm	0	[P50C]	Atkinson

Photolysis:

λ for the UV Bulb experiment will be 253 nm and 185 nm
input file "BULB"
$E_{Photon}=590*10^{-21}$ J/Photon

Actinic Flux: $J(253)=1.14*10^{16}$ Photons/(cm^2*s)
$J(185)=3.52*10^{14}$ Photons/(cm^2*s)

$HCHO+h\nu \rightarrow H^*+HCO^*$	λ<300nm	1.30E-5s $^{-1}$	[P1A]	Atkinson
$HCHO+h\nu \rightarrow CO+H_2$	λ≥300nm	2.16E-5 s^{-1}	[P1B]	Atkinson
$CH_3OH+h\nu \rightarrow$ negligible			[P2]	-----
$O_3+h\nu \rightarrow O(^1D)+O_2$	λ≤411nm	1.12E-1 s^{-1}	[P3A]	Atkinson
$O_3+h\nu \rightarrow O(^3P)+O_2$	λ<1180nm	1.32E-2 s^{-1}	[P3B]	Atkinson
$O_2+h\nu \rightarrow O(^1D)+O(^3P)$	λ<175nm	0	[P4A]	Atkinson
$O_2+h\nu \rightarrow O(^3P)+O(^3P)$	λ<242nm	1.23E-9 s^{-1}	[P4B]	Johnson/ Atkinson
$O_2+h\nu \rightarrow O(^1D)+O(^1D)$	λ<137nm	0	[P4C]	Johnson/ Atkinson
$H_2O_2+h\nu \rightarrow OH^*+OH^*$	λ<557nm	8.38E-4 s^{-1}	[P5A]	Atkinson
$H_2O_2+h\nu \rightarrow H_2O+O(^1D)$	λ<359nm	0, (Φ = 0)	[P5B]	Atkinson
$H_2O_2+h\nu \rightarrow H^*+HO_2^*$	λ<324nm	0, (Φ = 0)	[P5C]	Atkinson
$H_2O_2+h\nu \rightarrow 2H^*+O_2$	λ<213nm	0, (Φ = 0)	[P5D]	Atkinson
$NO_2+h\nu \rightarrow NO+O(^1D)$	λ≤244nm	0, (Φ = 0)	[P6A]	Atkinson
$NO_2+h\nu \rightarrow NO+O(^3P)$	λ<398nm	2.47E-4 s^{-1}	[P6B]	Atkinson
$H_2O+h\nu \rightarrow H_2+O(^3P)$	λ<243nm	0, (Φ = 0)	[P7A]	Atkinson
$H_2O+h\nu \rightarrow H^*+OH^*$	λ<239nm	1.09E-5 s^{-1}	[P7B]	Atkinson
$H_2O+h\nu \rightarrow H_2+O(^1D)$	λ<176nm	0	[P7C]	Atkinson
$CO_2+h\nu \rightarrow CO+O(^1D)$		negligible		
$CO_2+h\nu \rightarrow CO+O(^3P)$		negligible		
$HONO+h\nu \rightarrow NO+OH^*$	λ<591nm	1.69E-3 s^{-1}	[P50A]	Atkinson
$HONO+h\nu \rightarrow H^*+NO_2$	λ<367nm	0, (Φ = 0)	[P50B]	Atkinson
$HONO+h\nu \rightarrow HNO^*+O(^3P)$	λ<283nm	0, (Φ = 0)	[P50C]	Atkinson

Photolysis:

λ for the UV Bulb and the laser experiment will be 337, 253, and 185 nm
input file "COMBO"
$E_{Photon}=590*10^{-21}$ J/Photon

Actinic Flux: $J(337)=20.0*10^{15}$ Photons/(cm^2*s)
$J(253)=1.14*10^{16}$ Photons/(cm^2*s)
$J(185)=3.52*10^{14}$ Photons/(cm^2*s)

$HCHO+h\nu \rightarrow H^*+HCO^*$	λ<300nm	1.30E-5s $^{-1}$	[P1A]	Atkinson
$HCHO+h\nu \rightarrow CO+H_2$	λ≥300nm	3.86E-5 s^{-1}	[P1B]	Atkinson
$CH_3OH+h\nu \rightarrow$ negligible			[P2]	-----
$O_3+h\nu \rightarrow O(^1D)+O_2$	λ≤411nm	1.12E-1 s^{-1}	[P3A]	Atkinson
$O_3+h\nu \rightarrow O(^3P)+O_2$	λ<1180nm	1.32E-2 s^{-1}	[P3B]	Atkinson
$O_2+h\nu \rightarrow O(^1D)+O(^3P)$	λ<175nm	0	[P4A]	Atkinson
$O_2+h\nu \rightarrow O(^3P)+O(^3P)$	λ<242nm	1.23E-9 s^{-1}	[P4B]	Johnson/ Atkinson
$O_2+h\nu \rightarrow O(^1D)+O(^1D)$	λ<137nm	0	[P4C]	Johnson/ Atkinson
$H_2O_2+h\nu \rightarrow OH^*+OH^*$	λ<557nm	8.52E-4 s^{-1}	[P5A]	Atkinson
$H_2O_2+h\nu \rightarrow H_2O+O(^1D)$	λ<359nm	0, (Φ = 0)	[P5B]	Atkinson
$H_2O_2+h\nu \rightarrow H^*+HO_2^*$	λ<324nm	0, (Φ = 0)	[P5C]	Atkinson
$H_2O_2+h\nu \rightarrow 2H^*+O_2$	λ<213nm	0, (Φ = 0)	[P5D]	Atkinson
$NO_2+h\nu \rightarrow NO+O(^1D)$	λ≤244nm	0, (Φ = 0)	[P6A]	Atkinson
$NO_2+h\nu \rightarrow NO+O(^3P)$	λ<398nm	7.42E-4 s^{-1}	[P6B]	Atkinson
$H_2O+h\nu \rightarrow H_2+O(^3P)$	λ<243nm	0, (Φ = 0)	[P7A]	Atkinson
$H_2O+h\nu \rightarrow H^*+OH^*$	λ<239nm	1.09E-5 s^{-1}	[P7B]	Atkinson
$H_2O+h\nu \rightarrow H_2+O(^1D)$	λ<176nm	0	[P7C]	Atkinson
$CO_2+h\nu \rightarrow CO+O(^1D)$		negligible		
$CO_2+h\nu \rightarrow CO+O(^3P)$		negligible		
$HONO+h\nu \rightarrow NO+OH^*$	λ<591nm	2.61E-3 s^{-1}	[P50A]	Atkinson
$HONO+h\nu \rightarrow H^*+NO_2$	λ<367nm	0, (Φ = 0)	[P50B]	Atkinson
$HONO+h\nu \rightarrow HNO^*+O(^3P)$	λ<283nm	0, (Φ = 0)	[P50C]	Atkinson

Radical Chemistry:

$OH^* + O_3 = HO_2^* + O_2$	$6.7*10^{-14}$	$cm^3\ molecule^{-1}\ s^{-1}$	[R1]	DeMore
$HO_2^* + O_3 = OH^* + 2O_2$	$2.0*10^{-15}$	$cm^3\ molecule^{-1}\ s^{-1}$	[R2]	DeMore
$NO + O_3 = NO_2 + O_2$	$1.8*10^{-14}$	$cm^3\ molecule^{-1}\ s^{-1}$	[R3]	DeMore
$NO_2 + O_3 = NO_3 + O_2$	$1.2*10^{-13}$	$cm^3\ molecule^{-1}\ s^{-1}$	[R4]	DeMore
$HCO^* + O_2 = HO_2^* + CO$	$5.6*10^{-12}$	$cm^3\ molecule^{-1}\ s^{-1}$	[R9]	Anatasi
$HCHO + OH^* = H^* + CO + H_2O$	$1.1*10^{-11}$	$cm^3\ molecule^{-1}\ s^{-1}$	[R10]	Seinfeld
$OH^* + OH^* = H_2O + O(^1D)$	$1.9*10^{-12}$	$cm^3\ molecule^{-1}\ s^{-1}$	[R11]	DeMore
$OH^* + HO_2^* = H_2O + O_2$	$1.1*10^{-10}$	$cm^3\ molecule^{-1}\ s^{-1}$	[R12]	Atkinson
$OH^* + H_2O_2 = H_2O + HO_2^*$	$1.7*10^{-12}$	$cm^3\ molecule^{-1}\ s^{-1}$	[R13]	DeMore
$NO_2 + OH^* = HNO_3$	$1.1*10^{-11}$	$cm^3\ molecule^{-1}\ s^{-1}$	[R14]	Seinfeld
$CO + OH^* = CO_2 + H^*$	$2.9*10^{-13}$	$cm^3\ molecule^{-1}\ s^{-1}$	[R15]	DeMore
$N + OH^* = NO + H^*$	$4.9*10^{-11}$	$cm^3\ molecule^{-1}\ s^{-1}$	[R16]	Atkinson
$HCHO + OH^* = H_2O + HCO$	$1.0*10^{-11}$	$cm^3\ molecule^{-1}\ s^{-1}$	[R17]	Atkinson
$H^* + O_2 = HO_2^*$	$1.2*10^{-12}$	$cm^3\ molecule^{-1}\ s^{-1}$	[R18]	Anatasi
$H^* + O_3 = OH^* + O_2$	$2.9*10^{-11}$	$cm^3\ molecule^{-1}\ s^{-1}$	[R19]	Anatasi
$HO_2^* + HO_2^* = H_2O_2 + O_2$	$1.6*10^{-12}$	$cm^3\ molecule^{-1}\ s^{-1}$	[R20]	DeMore
$NO + HO_2^* = NO_2 + OH^*$	$8.3*10^{-12}$	$cm^3\ molecule^{-1}\ s^{-1}$	[R22]	DeMore
$NO_2 + HO_2^* = HONO + O_2$	$1.4*10^{-14}$	$cm^3\ molecule^{-1}\ s^{-1}$	[R23]	Stockwell
$CO + HO_2^* = CO_2 + OH^*$	$1.9*10^{-32}$	$cm^3\ molecule^{-1}\ s^{-1}$	[R24]	Atkinson
$O(^1D) + N_2 = O(^3P) + N_2$	$1.8*10^{-11}$	$cm^3\ molecule^{-1}\ s^{-1}$	[R30]	DeMore
$O(^3P) + O_2 + M = O_3 + M$	$2.9*10^{-11}$	$cm^3\ molecule^{-1}\ s^{-1}$	[R31]	Seinfeld
$NO + O(^3P) + M = NO_2 + M$	$3.0*10^{-11}$	$cm^3\ molecule^{-1}\ s^{-1}$	[R32]	Atkinson
$NO_2 + O(^3P) = O_2 + NO$	$9.7*10^{-12}$	$cm^3\ molecule^{-1}\ s^{-1}$	[R33]	DeMore
$O(^3P) + O_3 = O_2 + O_2$	$9.5*10^{-15}$	$cm^3\ molecule^{-1}\ s^{-1}$	[R35]	DeMore
$O(^1D) + H_2O = OH^* + OH^*$	$2.2*10^{-10}$	$cm^3\ molecule^{-1}\ s^{-1}$	[R36]	DeMore
$O(^1D) + O_3 = O_2 + O(^3P) + O(^3P)$	$1.2*10^{-11}$	$cm^3\ molecule^{-1}\ s^{-1}$	[R37]	DeMore
$O(^1D) + O_2 = O(^3P) + O_2$	$4.0*10^{-11}$	$cm^3\ molecule^{-1}\ s^{-1}$	[R38]	DeMore
$N + O_2 = NO + O(^3P)$	$8.9*10^{-17}$	$cm^3\ molecule^{-1}\ s^{-1}$	[R39]	Atkinson
$N + O_3 = NO + O_2$	$1.0*10^{-16}$	$cm^3\ molecule^{-1}\ s^{-1}$	[R40]	Atkinson
$NO + OH^* = HONO$	$1.1*10^{-11}$	$cm^3\ molecule^{-1}\ s^{-1}$	[R51]	Atkinson
$HONO + OH^* = H_2O + NO_2$	$4.9*10^{-12}$	$cm^3\ molecule^{-1}\ s^{-1}$	[R52]	Atkinson
$CH_3OH + OH^* = 0.85\{CH_2OH^*\} + 0.15\{CH_3O^* + H_2O\}$	$7.8*10^{-13}$	$cm^3\ molecule^{-1}\ s^{-1}$	[R60]	Atkinson
$CH_2OH^* + O_2 = HCHO + HO_2^*$	$9.8*10^{-12}$	$cm^3\ molecule^{-1}\ s^{-1}$	[R61]	Atkinson
$CH_3O^* + O_2 = HCHO + HO_2^*$	$1.9*10^{-15}$	$cm^3\ molecule^{-1}\ s^{-1}$	[R62]	Atkinson

Formaldehyde Reactions (HCHO):

Photolysis:

$HCHO+h\nu \rightarrow H^*+HCO^*$	$\lambda<300nm$	1.30E-5s $^{-1}$	[P1A]	Seinfeld
$HCHO+h\nu \rightarrow CO+H_2$	$\lambda\geq300nm$	3.86E-5 s^{-1}	[P1B]	Seinfeld

Radical Chemistry:

$HCHO+OH^*=H^*+CO+H_2O$	$1.1*10^{-11}$ cm^3 $molecule^{-1}$ s^{-1}		[R10]	Seinfeld
$HCHO+OH^*=H_2O+HCO^*$	$1.0*10^{-11}$ cm^3 $molecule^{-1}$ s^{-1}		[R17]	Atkinson
$CH_2OH^*+O_2=HCHO+HO_2^*$	$9.8*10^{-12}$ cm^3 $molecule^{-1}$ s^{-1}		[R61]	Atkinson
$CH_3O^*+O_2=HCHO+HO_2^*$	$1.9*10^{-15}$ cm^3 $molecule^{-1}$ s^{-1}		[R62]	Atkinson

$d[HCHO]/dt=-P1A-P1B-R10-R17+R61+R62$

Methanol Reactions (CH_3OH):

Photolysis:

$CH_3OH+h\nu \rightarrow$ negligible			[P2]	

Radical Chemistry:

$CH_3OH+OH^*=0.85\{CH_2OH^*\}+0.15\{CH_3O^*+H_2O\}$	$7.8*10^{-13}$ cm^3 $molecule^{-1}$ s^{-1}		[R60]	Atkinson

$d[CH_3OH]/dt=-R60$

Carbon Dioxide Reactions (CO_2):

Radical Chemistry:

$CO + OH^* \rightarrow CO_2 + H^*$	$2.2*10^{-13}$ cm^3 $molecule^{-1}$ s^{-1}		[R15]	DeMore
$CO + HO_2^* \rightarrow CO_2 + OH^*$	$1.9*10^{-32}$ cm^3 $molecule^{-1}$ s^{-1}		[R24]	Atkinson

$d[CO_2]/dt=P15+P24$

Atomic Oxygen Reactions (O):

Photolysis:

$O_3+h\nu \rightarrow O(^1D)+O_2$	$\lambda \leq 411nm$	1.12E-1 s^{-1}	[P3A]	Atkinson
$O_3+h\nu \rightarrow O(^3P)+O_2$	$\lambda < 1180nm$	1.32E-2 s^{-1}	[P3B]	Atkinson
$O_2+h\nu \rightarrow O(^1D)+O(^3P)$	$\lambda < 175nm$	0	[P4A]	Atkinson
$O_2+h\nu \rightarrow O(^3P)+O(^3P)$	$\lambda < 242nm$	1.23E-9 s^{-1}	[P4B]	Atkinson
$O_2+h\nu \rightarrow O(^1D)+O(^1D)$	$\lambda < 137nm$	0	[P4C]	Atkinson
$NO_2+h\nu \rightarrow NO+O(^1D)$	$\lambda \leq 244nm$	0, ($\Phi = 0$)	[P6A]	Atkinson
$NO_2+h\nu \rightarrow NO+O(^3P)$	$\lambda < 398nm$	7.42E-4 s^{-1}	[P6B]	Atkinson
$H_2O+h\nu \rightarrow H_2+O(^3P)$	$\lambda < 243nm$	0, ($\Phi = 0$)	[P7A]	Atkinson
$H_2O+h\nu \rightarrow H_2+O(^1D)$	$\lambda < 176nm$	0	[P7C]	Atkinson
$H_2O_2+h\nu \rightarrow H_2O+O(^1D)$	$\lambda < 359nm$	0, ($\Phi = 0$)	[P5B]	Atkinson
$HONO+h\nu \rightarrow HNO^*+O(^3P)$	$\lambda < 283nm$	0, ($\Phi = 0$)	[P50C]	Atkinson

Radical Chemistry:

$OH^*+OH^*=H_2O+O(^1D)$	$1.9*10^{-12}$ cm^3 $molecule^{-1}$ s^{-1} [a]	[R11]	DeMore
$O(^1D)+N_2=O(^3P)+N_2$	$1.8*10^{-11}$ cm^3 $molecule^{-1}$ s^{-1}	[R30]	DeMore
$O(^3P)+O_2+M=O_3+M$	$2.9*10^{-11}$ cm^3 $molecule^{-1}$ s^{-1}	[R31]	Seinfeld
$NO+O(^3P)+M=NO_2+M$	$3.0*10^{-11}$ cm^3 $molecule^{-1}$ s^{-1}	[R32]	Atkinson
$NO_2+O(^3P)=O_2+NO$	$9.7*10^{-12}$ cm^3 $molecule^{-1}$ s^{-1}	[R33]	DeMore
$O(^3P)+O_3=2O_2$	$9.5*10^{-15}$ cm^3 $molecule^{-1}$ s^{-1}	[R35]	DeMore
$O(^1D)+H_2O=2OH^*$	$2.2*10^{-10}$ cm^3 $molecule^{-1}$ s^{-1}	[R36]	DeMore
$O(^1D)+O_3=O_2+2O(^3P)$	$1.2*10^{-11}$ cm^3 $molecule^{-1}$ s^{-1}	[R37]	DeMore
$O(^1D)+O_2=O(^3P)+O_2$	$4.0*10^{-11}$ cm^3 $molecule^{-1}$ s^{-1}	[R38]	DeMore
$N+O_2=NO+O(^3P)$	$8.9*10^{-17}$ cm^3 $molecule^{-1}$ s^{-1}	[R39]	Atkinson

[a]Assumed the products of R11 were negligible.

Use Steady State Assumption:

$$[O(^3P)]_{SS}=(P3B+P4A+P4B+P6B+P7A+P50C+R30+R37+R38+R39)/(KR33*NO_2*KR35*O_3+KR32*NO+KR31*O_2)$$

$$[O(^1D)]_{SS}=(P3A+P4A+P4C+P6A+P7C+P5B+R11)/(KR30*N_2+KR36*H2O+KR37*O_3+KR38*O_2)$$

NO Reactions:

Photolysis:

$NO_2+h\nu \rightarrow NO+O(^1D)$	$\lambda \leq 244nm$	0, ($\Phi = 0$)	[P6A]	Atkinson
$NO_2+h\nu \rightarrow NO+O(^3P)$	$\lambda < 398nm$	7.42E-4 s^{-1}	[P6B]	Atkinson
$HONO+h\nu \rightarrow NO+OH^*$	$\lambda < 591nm$	2.61E-3 s^{-1}	[P50A]	Atkinson

Radical Chemistry:

$NO + O_3 = NO_2 + O_2$	$1.8*10^{-14}$ cm^3 $molecule^{-1}$ s^{-1}	[R3]	DeMore
$N + OH^* = NO + H^*$	$4.9*10^{-11}$ cm^3 $molecule^{-1}$ s^{-1}	[R16]	Atkinson
$NO + HO_2^* = NO_2 + OH^*$	$8.3*10^{-12}$ cm^3 $molecule^{-1}$ s^{-1}	[R22]	DeMore
$NO + O(^3P) + M = NO_2 + M$	$3.0*10^{-11}$ cm^3 $molecule^{-1}$ s^{-1}	[R32]	Atkinson
$NO_2 + O(^3P) = O_2 + NO$	$9.7*10^{-12}$ cm^3 $molecule^{-1}$ s^{-1}	[R33]	DeMore
$N+O_2=NO+O(^3P)$	$8.9*10^{-17}$ cm^3 $molecule^{-1}$ s^{-1}	[R39]	Atkinson
$N+O_3=NO+O_2$	$1.0*10^{-16}$ cm^3 $molecule^{-1}$ s^{-1}	[R40]	Atkinson
$NO+OH^*=HONO$	$1.1*10^{-11}$ cm^3 $molecule^{-1}$ s^{-1}	[R51]	Atkinson

$d[NO]/dt=P6A+P6B+P50A-R3+R16-R22-R32+R33+R39+R40-R51$

Hydrogen Peroxide Reactions (H_2O_2):

Photolysis:

$H_2O_2 + h\nu \rightarrow OH^* + OH^*$	$\lambda < 577$ nm	8.52E-4 s^{-1}	[P5A]	Atkinson
$H_2O_2 + h\nu \rightarrow H_2O + O(^1D)$	$\lambda < 359$ nm	0, ($\Phi = 0$)	[P5B]	Atkinson
$H_2O_2 + h\nu \rightarrow H^*+HO_2^*$	$\lambda < 324$ nm	0, ($\Phi = 0$)	[P5C]	Atkinson
$H_2O_2 + h\nu \rightarrow 2H^*+O_2$	$\lambda < 213$ nm	0, ($\Phi = 0$)	[P5D]	Atkinson

Radical Chemistry:

$OH^* + H_2O_2 = H_2O + HO_2^*$	$1.7*10^{-12}$ cm^3 $molecule^{-1}$ s^{-1}	[R13]	DeMore
$HO_2^* + HO_2^* = H_2O_2 + O_2$	$1.6*10^{-12}$ cm^3 $molecule^{-1}$ s^{-1}	[R20]	DeMore

$d[H_2O_2]/dt=-P5A-P5B-P5C-P5D-R13+R20$

NO_2 Reactions:

Photolysis:

$NO_2+h\nu \rightarrow NO+O(^1D)$	$\lambda \leq 244nm$	0, ($\Phi = 0$)	[P6A]	Atkinson
$NO_2+h\nu \rightarrow NO+O(^3P)$	$\lambda < 398nm$	7.42E-4 s^{-1}	[P6B]	Atkinson
$HONO+h\nu \rightarrow H^*+NO_2$	$\lambda < 367nm$	0, ($\Phi = 0$)	[P50B]	Atkinson

Radical Chemistry:

$NO+O_3=NO_2+O_2$	$1.8*10^{-14}$ cm^3 $molecule^{-1}$ s^{-1}	[R3]	DeMore
$NO_2+O_3=NO_3+O_2$	$1.2*10^{-13}$ cm^3 $molecule^{-1}$ s^{-1}	[R4]	DeMore
$NO_2+OH^*=HNO_3$	$1.1*10^{-11}$ cm^3 $molecule^{-1}$ s^{-1}	[R14]	Seinfeld
$NO+HO_2^*=NO_2+OH^*$	$8.3*10^{-12}$ cm^3 $molecule^{-1}$ s^{-1}	[R22]	DeMore
$NO_2+HO_2^*=HONO+O_2$	$1.4*10^{-12}$ cm^3 $molecule^{-1}$ s^{-1}	[R23]	Stockwell
$NO+O(^3P)+M=NO_2+M$	$3.0*10^{-11}$ cm^3 $molecule^{-1}$ s^{-1}	[R32]	Atkinson
$NO_2+O(^3P)=O_2+NO$	$9.7*10^{-12}$ cm^3 $molecule^{-1}$ s^{-1}	[R33]	DeMore
$HONO+OH^*=H_2O+NO_2$	$4.9*10^{-12}$ cm^3 $molecule^{-1}$ s^{-1}	[R52]	Atkinson

$d[NO_2]/dt$=-P6A-P6B+P50B+R3-R4-R14+R22-R23+R32-R33+R52

Nitrous Acid Reactions (HONO):

Photolysis:

$HONO+h\nu \rightarrow NO+OH^*$	$\lambda < 591nm$	2.61E-3 s^{-1}	[P50A]	Atkinson
$HONO+h\nu \rightarrow H^*+NO_2$	$\lambda < 367nm$	0, ($\Phi = 0$)	[P50B]	Atkinson
$HONO+h\nu \rightarrow HNO^*+O(^3P)$	$\lambda < 283nm$	0, ($\Phi = 0$)	[P50C]	Atkinson

Radical Chemistry:

$NO_2+HO_2^*=HONO+O_2$	$1.4*10^{-14}$ cm^3 $molecule^{-1}$ s^{-1}	[R23]	Stockwell
$NO+OH^*=HONO$	$1.1*10^{-11}$ cm^3 $molecule^{-1}$ s^{-1}	[R51]	Atkinson
$HONO+OH^*=H_2O+NO_2$	$4.9*10^{-12}$ cm^3 $molecule^{-1}$ s^{-1}	[R52]	Atkinson

$d[HONO]/dt$=-P50A-P50B-P50C+R23+R51-R52

Hydroxyl Radical Reactions (OH*):

Photolysis:

$H_2O_2+h\nu \rightarrow OH^*+OH^*$	$\lambda<557nm$	$8.52E\text{-}4\ s^{-1}$	[P5A]	Atkinson
$H_2O+h\nu \rightarrow H^*+OH^*$	$\lambda<239nm$	$1.09E\text{-}5\ s^{-1}$	[P7B]	Atkinson
$HONO+h\nu \rightarrow NO+OH^*$	$\lambda<591nm$	$2.61E\text{-}3\ s^{-1}$	[P50A]	Atkinson

Radical Chemistry:

$OH^*+O_3=HO_2^*+O_2$	$6.7*10^{-14}$ $cm^3\ molecule^{-1}\ s^{-1}$	[R1]	DeMore
$HO_2^*+O_3=OH^*+2O_2$	$2.0*10^{-15}$ $cm^3\ molecule^{-1}\ s^{-1}$	[R2]	DeMore
$HCHO+OH^*=H^*+CO+H_2O$	$1.1*10^{-11}$ $cm^3\ molecule^{-1}\ s^{-1}$	[R10]	Seinfeld
$OH^*+OH^*=H_2O+O(^1D)$	$1.9*10^{-12}$ $cm^3\ molecule^{-1}\ s^{-1}$ [b]	[R11]	DeMore
$OH^*+HO_2^*=H_2O+O_2$	$1.1*10^{-10}$ $cm^3\ molecule^{-1}\ s^{-1}$	[R12]	Atkinson
$OH^*+H_2O_2=H_2O+HO_2^*$	$1.7*10^{-12}$ $cm^3\ molecule^{-1}\ s^{-1}$	[R13]	DeMore
$NO_2+OH^*=HNO_3$	$1.1*10^{-11}$ $cm^3\ molecule^{-1}\ s^{-1}$	[R14]	Seinfeld
$CO+OH^*=CO_2+H^*$	$2.2*10^{-13}$ $cm^3\ molecule^{-1}\ s^{-1}$	[R15]	DeMore
$N+OH^*=NO+H^*$	$4.9*10^{-11}$ $cm^3\ molecule^{-1}\ s^{-1}$	[R16]	Atkinson
$H^*+O_3 = OH^*+O_2$	$2.9*10^{-11}$ $cm^3\ molecule^{-1}\ s^{-1}$	[R19]	Anatasi
$NO+HO_2^*=NO_2+OH^*$	$8.3*10^{-12}$ $cm^3\ molecule^{-1}\ s^{-1}$	[R22]	DeMore
$CO+HO_2^*=CO_2+OH^*$	$1.9*10^{-32}$ $cm^3\ molecule^{-1}\ s^{-1}$	[R24]	Atkinson
$O(^1D)+H_2O=OH^*+OH^*$	$2.2*10^{-10}$ $cm^3\ molecule^{-1}\ s^{-1}$	[R36]	DeMore
$NO+OH^*=HONO$	$1.1*10^{-12}$ $cm^3\ molecule^{-1}\ s^{-1}$	[R51]	Atkinson
$HONO+OH^*=H_2O+NO_2$	$6.6*10^{-12}$ $cm^3\ molecule^{-1}\ s^{-1}$	[R52]	Atkinson
$CH_3OH+OH^*=0.85\{CH_2OH^*\}+0.15\{CH_3O^*+H_2O\}$	$7.8*10^{-13}$ $cm^3\ molecule^{-1}\ s^{-1}$	[R60]	Atkinson

[b] Assumed [OH*] to be low, considered R11 to be negligible.

Use Steady State Assumption:

$$[OH^*]_{SS}=(P5A+P7B+P50A+R2+R19+R22+R24+2*R36)/(KR1*O_3+KR10*HCHO+KR12*HO_2+KR13*H_2O_2+KR14*NO_2+KR15*CO+KR16*N+KR51*NO+KR52*HONO+KR60*CH_3OH)$$

Hydroperoxyl Radical Reactions (HO_2*):

Photolysis:

$H_2O_2+h\nu \rightarrow H^*+HO_2^*$	$\lambda<324nm$	0, ($\Phi=0$)	[P5C]	Atkinson

Radical Chemistry:

$OH^*+O_3=HO_2^*+O_2$	$6.7*10^{-14}$ cm^3 $molecule^{-1}$ s^{-1}	[R1]	DeMore
$HO_2^*+O_3=OH^*+2O_2$	$2.0*10^{-15}$ cm^3 $molecule^{-1}$ s^{-1}	[R2]	DeMore
$HCO^*+O_2=HO_2^*+CO$	$5.6*10^{-12}$ cm^3 $molecule^{-1}$ s^{-1}	[R9]	Anatasi
$OH^*+H_2O_2=H_2O+HO_2^*$	$1.7*10^{-12}$ cm^3 $molecule^{-1}$ s^{-1}	[R13]	Seinfeld
$H^*+O_2=HO_2^*$	$1.2*10^{-12}$ cm^3 $molecule^{-1}$ s^{-1}	[R18]	Anatasi
$HO_2^*+HO_2^*=H_2O_2+O_2$	$1.6*10^{-12}$ cm^3 $molecule^{-1}$ s^{-1} c	[R20]	Seinfeld
$NO+HO_2^*=NO_2+OH^*$	$8.3*10^{-12}$ cm^3 $molecule^{-1}$ s^{-1}	[R22]	Seinfeld
$NO_2+HO_2^*=HONO+O_2$	$1.4*10^{-14}$ cm^3 $molecule^{-1}$ s^{-1}	[R23]	Stockwell
$CO+HO_2^*=CO_2+OH^*$	$1.9*10^{-32}$ cm^3 $molecule^{-1}$ s^{-1}	[R24]	Atkinson

[c]Assumed [HO_2] to be low, considered R20 to be negligible.

Use Steady State Assumption:

$[HO_2^*]_{SS}=(P5C+R1+R9+R13+R18)/(KR2*O_3+KR22*NO+KR23*NO_2+KR24*CO)$

Carbon Monoxide Reactions (CO):

Photolysis:

$HCHO+h\nu \rightarrow CO+H_2$	$\lambda>300nm$	3.86E-5 s^{-1}	[P1B]	Atkinson

Radical Chemistry:

$HCO^*+O_2=HO_2^*+CO$	$5.6*10^{-12}$ cm^3 $molecule^{-1}$ s^{-1}	[R9]	Anatasi
$HCHO+OH^*= H^*+CO+H_2O$	$1.1*10^{-11}$ cm^3 $molecule^{-1}$ s^{-1}	[R10]	Seinfeld
$CO+OH^*= CO_2+H^*$	$2.2*10^{-13}$ cm^3 $molecule^{-1}$ s^{-1}	[R15]	DeMore
$CO+HO_2^*= CO_2+OH^*$	$1.9*10^{-32}$ cm^3 $molecule^{-1}$ s^{-1}	[R24]	Atkinson

$d[CO]/dt=P1B+R9+R10-R15-R24$

Atomic Hydrogen Reactions (H*):

Photolysis:

$HCHO+h\nu \rightarrow H^*+HCO^*$	$\lambda<300nm$	$1.30E\text{-}5s^{-1}$	[P1A]	Atkinson
$H_2O_2+h\nu \rightarrow H^*+HO_2^*$	$\lambda<324nm$	$0, (\Phi = 0)$	[P5C]	Atkinson
$H_2O_2+h\nu \rightarrow 2H^*+O_2$	$\lambda<213nm$	$0, (\Phi = 0)$	[P5D]	Atkinson
$H_2O+h\nu \rightarrow H^*+OH^*$	$\lambda<239nm$	$1.09E\text{-}5\ s^{-1}$	[P7B]	Atkinson
$HONO+h\nu \rightarrow H^*+NO_2$	$\lambda<367nm$	$0, (\Phi = 0)$	[P50B]	Atkinson

Radical Chemistry:

$HCHO+OH^*=H^*+CO+H_2O$	$1.1*10^{-11}$	$cm^3\ molecule^{-1}\ s^{-1}$	[R10]	Seinfeld
$CO+OH^*=CO_2+H^*$	$2.9*10^{-13}$	$cm^3\ molecule^{-1}\ s^{-1}$	[R15]	DeMore
$N+OH^*=NO+H^*$	$4.9*10^{-11}$	$cm^3\ molecule^{-1}\ s^{-1}$	[R16]	Atkinson
$H^*+O_2 = HO_2^*$	$1.2*10^{-12}$	$cm^3\ molecule^{-1}\ s^{-1}$	[R18]	Anatasi
$H^*+O_3 = OH^*+ O_2$	$2.9*10^{-11}$	$cm^3\ molecule^{-1}\ s^{-1}$	[R19]	Anatasi

$d[H^*]/dt=P1A+P5C+P5B+P7B+P50B+R10+R15+R16-R18-R19$

Formyl Radical Reactions (HCO*):

Photolysis:

$HCHO+h\nu \rightarrow H^*+HCO^*$	$\lambda<300nm$	$1.30E\text{-}5s^{-1}$	[P1A]	Atkinson

Radical Chemistry:

$HCO^*+O_2 = HO_2^*+CO$	$5.6*10^{-12}$	$cm^3\ molecule^{-1}\ s^{-1}$	[R9]	Anatasi
$HCHO+OH^*= H_2O+HCO^*$	$1.0*10^{-11}$	$cm^3\ molecule^{-1}\ s^{-1}$	[R17]	Atkinson

$d[HCO^*]/dt=P1A-R9+R17$

Atmospheric Gases: [Seinfeld, p. 8]

Gas	Avg. Concentration[ppm]
Ar	9340
Ne	18
Kr	1.1
Xe	0.09
N_2	780,840
O_2	209,460
CH_4	1.65
CO_2	332
CO	0.05-0.2
H_2	0.58
N_2O	0.33
SO_2	10^{-5}-10^{-4}
NH_3	10^{-4}-10^{-3}
$NO+NO_2$	10^{-6}-10^{-2}
O_3	10^{-2}-10^{-1}
HNO_3	10^{-5}-10^{-3}
OH	$0.406*10^{-5}$ ppb
HO_2	$0.406*10^{-2}$ ppb
O_3	30 ppb
H_2O_2	10 ppb
H_2O	22,550
He	5.2